polymer reviews

Structure and properties of crystalline polymers

Hiroyuki Tadokoro
Department of Macromolecular Science, Faculty of Science, Osaka University, Toyonaka, Osaka 560, Japan
(Received 3 May 1983)

Starting with a structural study of the crystallization behaviour of poly(vinyl alcohol), the author has been analysing the crystal and molecular structures of crystalline polymers for the past 35 years. One of the characteristic points of the methods used is the co-operative use of X-ray diffraction and infrared and Raman spectroscopy (normal coordinate treatment). There are many examples of the application of this technique to a series of polyethers, polythioethers, polyesters, polymer complexes etc. Furthermore, the intra- and intermolecular energy calculations have succeeded in accelerating the structural analyses of important but complicated polymer materials and in revealing the factors governing the stable crystal structure and molecular conformation of a polymer. Poly(ethylene oxybenzoate) α form and double-stranded helices of *isotactic* poly(methyl methacrylate), the first double helix ever found for synthetic polymers, are used as typical for the application of this method. The structural interpretation of the mechanism of optical compensation in racemic polymers is also a good example. The energy calculations have developed to the stage where the stability of two crystal forms of polyethylene can be discussed in terms of free energy. Utilizing the structural data thus accumulated and the spectroscopically obtained interaction parameters, the structure–property relationship has been clarified quantitatively by lattice dynamical theory. The calculated crystallite moduli of polymer chains agree well with the observed ones for many polymers such as poly-*p*-phenylene terephthalamide, etc. The study has been advanced by a new method of calculation of the three-dimensional elastic constant tensor and its application to polyethylene, poly(vinyl alcohol), nylon 6 etc. As an extension the general method of calculating the piezoelectric constant tensor has also been derived and successfully applied to poly(vinylidene fluoride) form I, resulting in the interpretation of the origin of macroscopic piezoelectricity of this polymer.

Keywords: Polymers; crystal structure; molecular conformation; X-ray analysis; infrared and Raman spectra; normal coordinate treatments; energy calculations; elasticity; piezoelectricity

INTRODUCTION

In this paper I discuss the structure and properties of crystalline polymers, the theme of which has been my life work for the past thirty-five years. The first topic concerns structural analyses of crystalline polymers by the organized utilization of X-ray diffraction, infrared and Raman spectroscopy, and the energy calculations. Secondly I discuss the quantitative understanding of the relation between structure and properties of polymers.

Although this paper may be in a form of a rather autobiographical scientific review, the author will be fortunate if it could give the readers some benefit as a guide for carrying out structural research of crystalline polymers.

OUR EARLY STUDIES ON STRUCTURE OF CRYSTALLINE POLYMERS

I started my scientific work on polymer materials in 1950. For nearly seven years I was engaged in the study of crystallization behaviour of poly(vinyl alcohol) (PVA) by measuring sorption of water vapour, density, infrared absorption, and X-ray diffraction[1,2]. It was through this work that I became captivated by crystallization-sensitive infrared bands. Among the vibrational bands of *atactic* PVA, the 1141 cm^{-1} band is very sensitive to the variation of crystallinity of the sample. We could assign this band to the symmetric skeletal stretching mode by the various experimental techniques such as deuteration, double orientation, infrared microspectroscopic measurements, etc.[3,4] This band assignment was confirmed 26 years later by the measurements of polarized Raman spectra of a double-oriented *atactic* PVA sample (*Figure 1*)[5].

In 1958 I began infrared studies of stereoregular polymers and found the infrared bands inherent in the helical structures of *isotactic* polystyrene and related polymers[6-8]. From the pursuit of the origin of infrared bands associated with the helical structure, I naturally went into X-ray structure analysis and normal coordinate treatment of polyoxymethylene [–(CH_2–O–)–; POM], a helical polymer with monomeric units simpler than *isotactic* polystyrene.

Polyoxymethylene

At that time the structure of POM had not been clarified and two possible structural models of (9/5) and (9/4) helices had been proposed. Here (9/5) means nine monomeric units turn five times in the fibre identity period of 17.3 Å, as shown in *Figure 2*. Huggins proposed qualitatively the (9/5) helix[9] and the other investigators supported the (9/4) helical model[10]. Based on the X-ray diffraction data shown in *Figure 3*, where the upper

0032-3861/84/020147-18$03.00

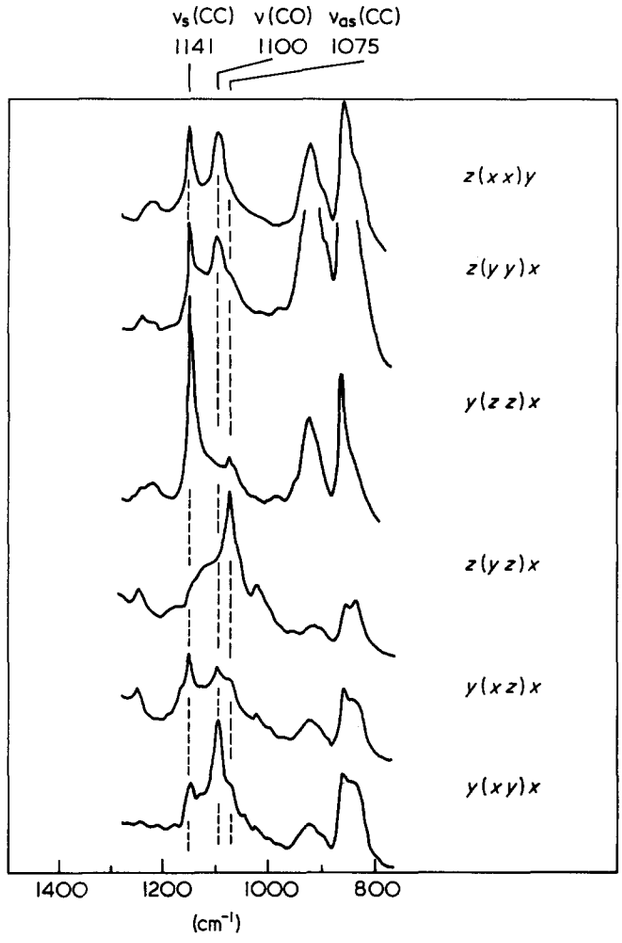

Figure 1 Polarized Raman spectra of doubly oriented *atactic* poly(vinyl alcohol)[5]

photograph is the fibre diagram of POM obtained from solid-state polymerization of tetraoxane single crystals and the lower one is for the uniaxially oriented Delrin acetal resin, we could determine the molecular structure to be a (9/5) helix[11-14].

Based on this X-ray structural analysis, we tried to assign the infrared and Raman bands by carrying out the normal coordinate treatments; the general equation of calculating the normal vibrational modes of helical polymer chains was derived[15,16], and applied successfully to POM[17,18]. In *Figures 4* and *5* are shown, respectively, the polarized infrared spectra and Raman spectra of POM and deuterated POM, where the Raman spectra were measured using a mercury lamp, not a laser beam, as a light source.

Poly(ethylene oxide)

Since 1964 I had advanced my work widely to the various types of polymers, among which there was a series of polyethers $[-(CH_2)_m-O-]_n$; poly(ethylene oxide) [$m=2$, PEO], poly(oxacyclobutane) ($m=3$) etc.[19-27].

For PEO we proposed in 1961 a molecular model of (7/2) helix as shown in *Figure 2*, based on the information from X-ray diffraction, infrared and Raman spectroscopy, and also the preparation of deuterated polymer samples[19,20]. But at that time we could not determine the crystal structure. We developed the methods of X-ray structural analysis, especially the constrained least squares method for calculation of structure factors[28] which was a refinement of the original one first proposed by Arnott and Wonacott[29], and produced a vacuum cylindrical camera with radius 10 cm (*Figure 6*), which gives clear separation of reflections and no air scattering. In *Figure 7* is shown the X-ray fibre diagram of PEO taken by this large vacuum camera[30]. Utilizing these techniques the crystal structure of PEO has been determined, as shown in *Figure 8*, 10 years after the uniform helical model of (7/2) was proposed[30]. The helix is considerably distorted from the uniform one.

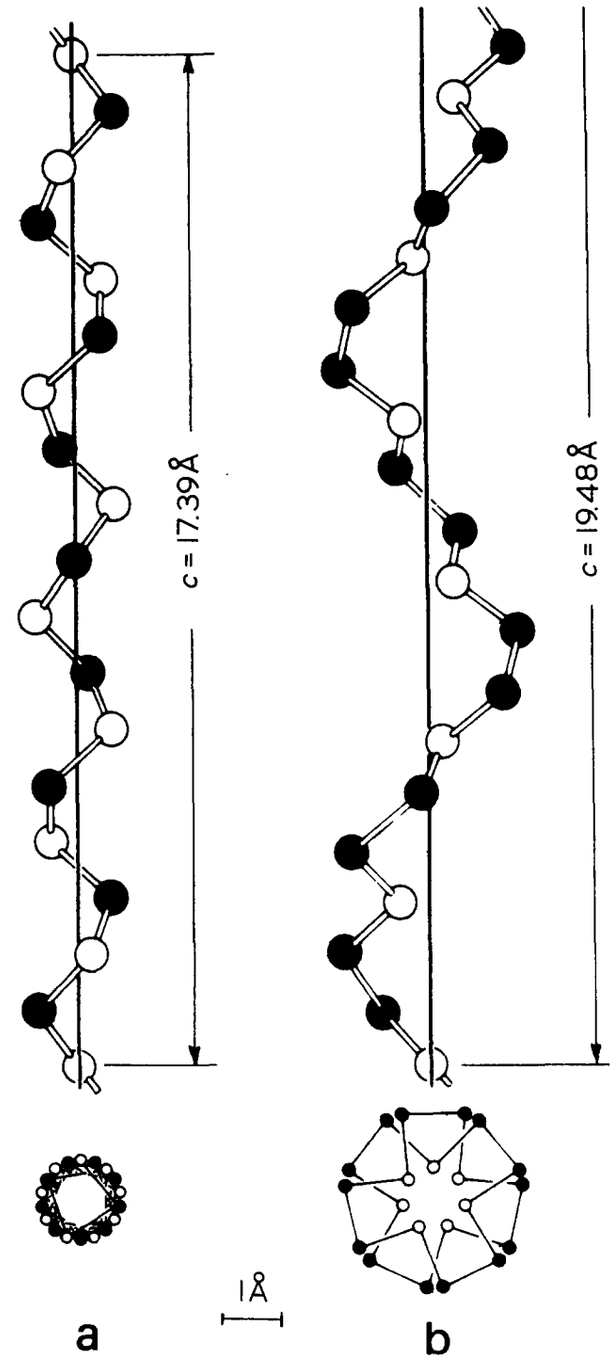

Figure 2 Molecular structures of (a) polyoxymethylene and (b) poly(ethylene oxide)[12]

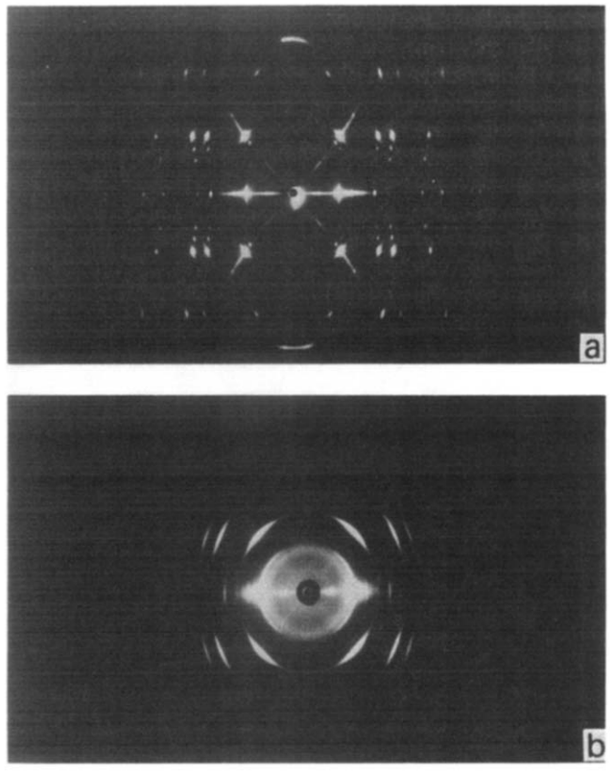

Figure 3 X-ray fibre diagram of polyoxymethylene samples.[12,13] (a) Polyoxymethylene obtained from solid-state polymerization of tetraoxane single crystals; (b) uniaxially oriented Delrin acetal resin

The molecular distortion of our new model is appreciable, but the conformation is essentially the (7/2) helix and close to the TTG repeating sequences of a uniform helical model. At that time when we proposed the uniform helical model, Flory independently clarified the stable conformation of PEO in solution as TTG[31]. In 1964 I met him and we found that our results in solution and in solid were consistent with each other.

To clarify the reason for the distortion of the helix, we developed a packing energy minimization method[32]. Starting from a crystal structure model consisting of the uniform (7/2) helices, the minimal point of packing energy was searched by taking into account the intermolecular interactions. The resultant structure model is shown in

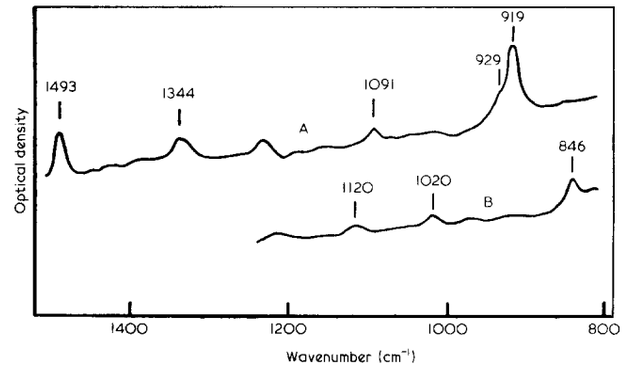

Figure 5 Raman spectra of A, polyoxymethylene; and B, polyoxymethylene-d_2 [18]

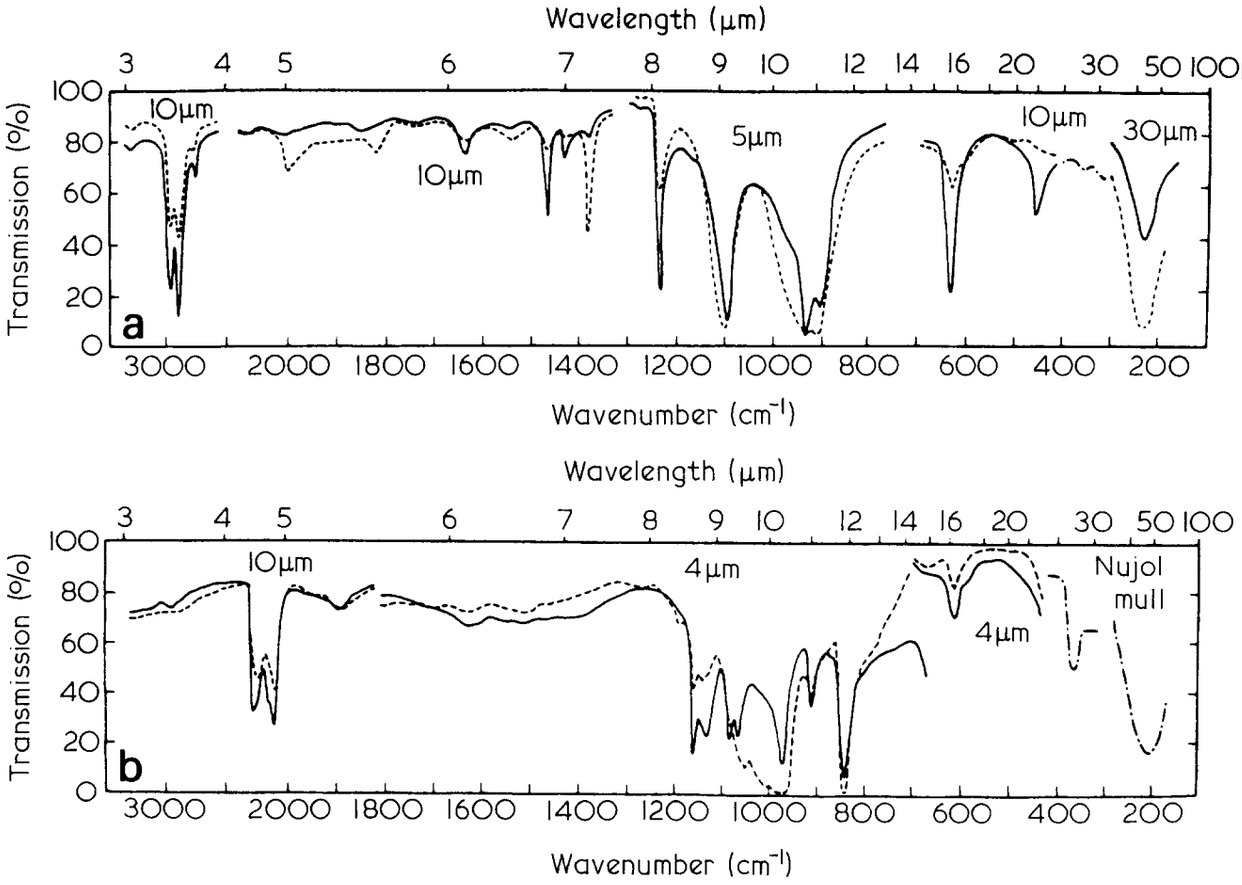

Figure 4 Polarized infrared spectra of (a) polyoxymethylene; and (b) polyoxymethylene-d_2.[18] ———, Electric vector perpendicular to elongation axis; – – –, electric vector parallel to elongation axis

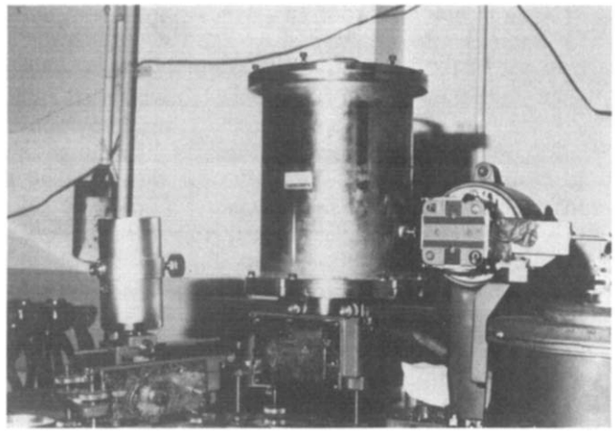

Figure 6 Vacuum cylindrical camera with a radius 10 cm.[94] The small camera on the left has a radius 3.5 cm

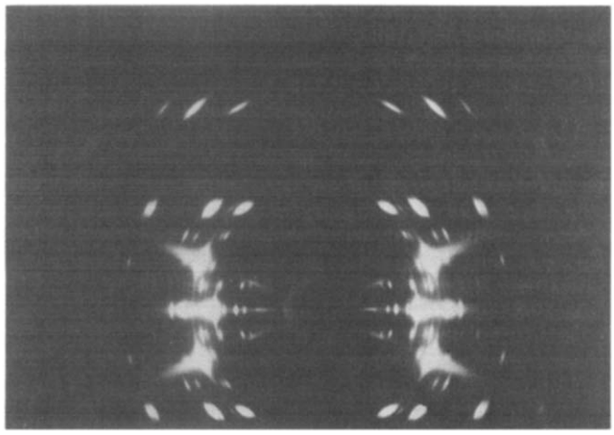

Figure 7 X-ray fibre diagram of poly(ethylene oxide) taken with the vacuum cylindrical camera shown in *Figure 6*[30]

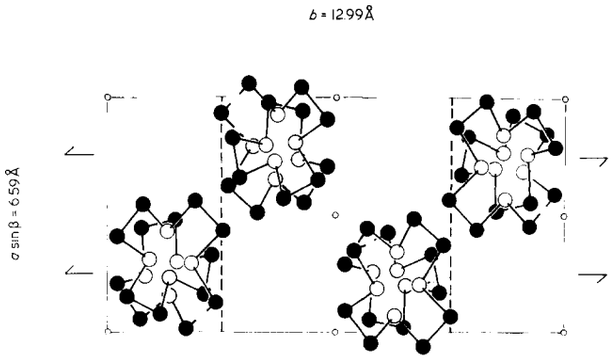

Figure 8 Crystal structure of poly(ethylene oxide)[30]

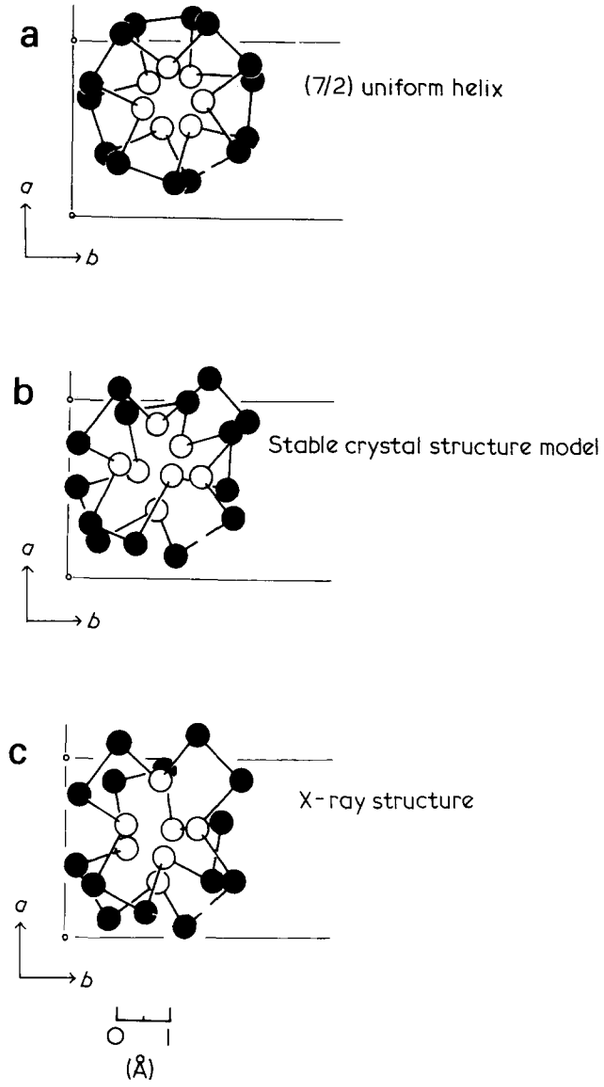

Figure 9 Crystal structure model of poly(ethylene oxide).[32] (a) Starting uniform helical model; (b) stable crystal structure model obtained by the energy minimization; (c) the structure determined by X-ray analysis

Figure 9b, which is in a reasonably good agreement with the structure determined by X-ray analysis (*Figure 9c*). This suggests that the deformation of the PEO chain from a uniform helix in the crystal lattice is principally due to the intermolecular interactions.

Polyisobutylene

Polyisobutylene gives a beautiful fibre diagram as shown in *Figure 10*, the structure analysis of which had been established prior to this by many scientists including Bunn[33], but the structure still had not been determined

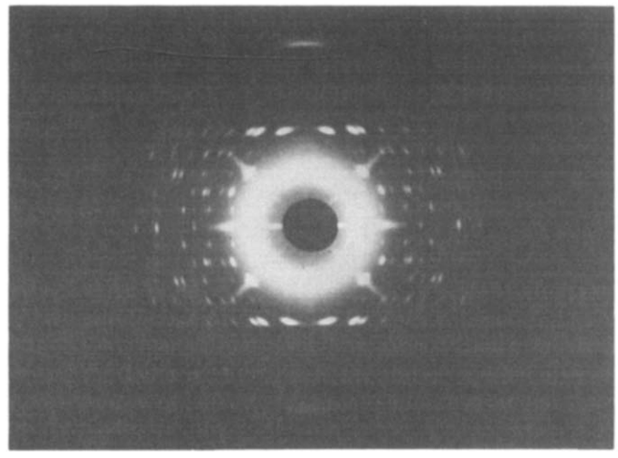

Figure 10 X-ray fibre diagram of polyisobutylene[34]

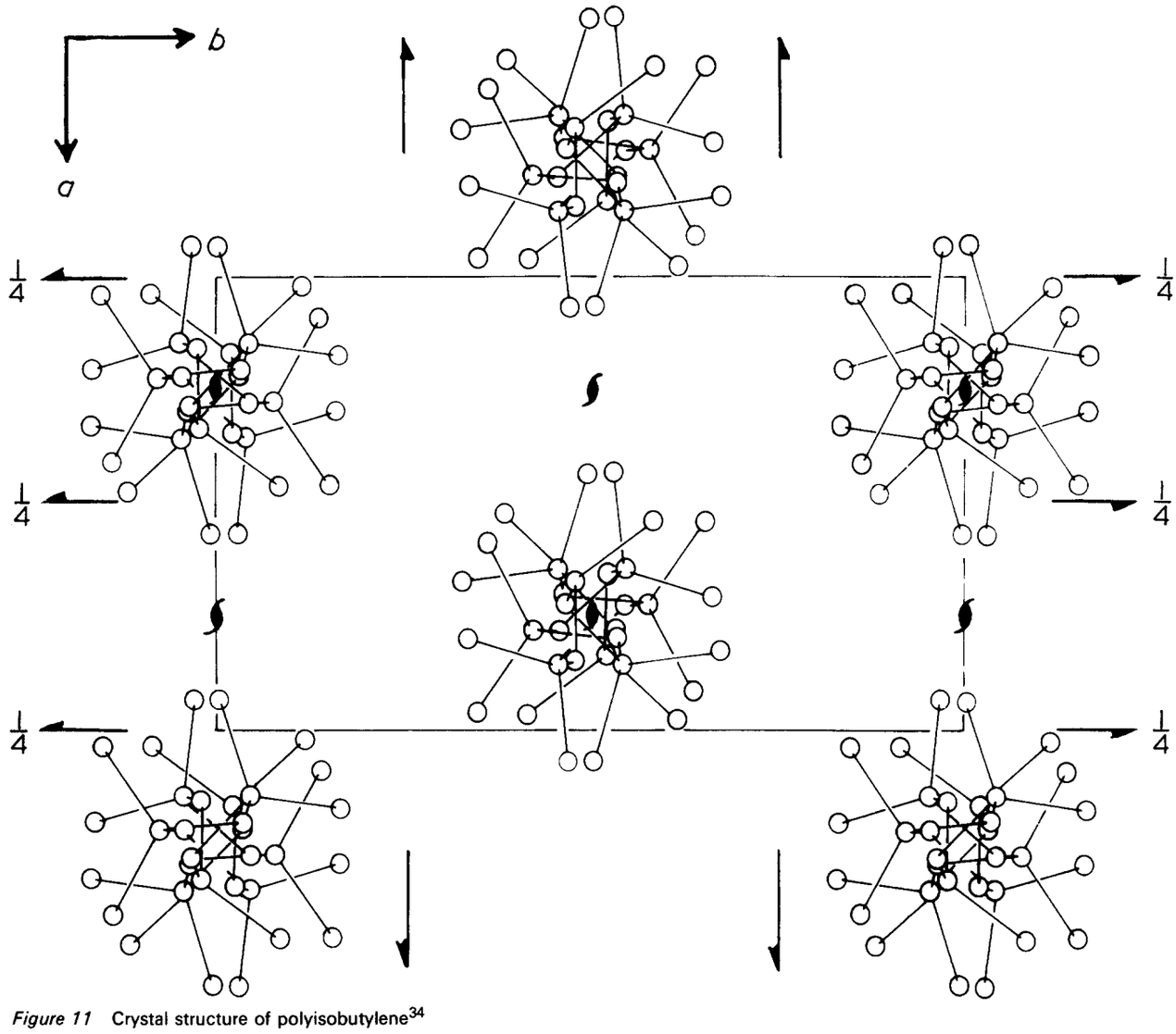

Figure 11 Crystal structure of polyisobutylene[34]

clearly. When I visited Dr Bunn in London, he recommended kindly the structure analysis of this polymer to us. And finally we could determine the crystal structure as shown in *Figure 11*[34]. The molecular structure is approximately a (8/3) helix but is distorted more or less by the intermolecular interactions. The chain has only a 2_1 screw symmetry and a crystallographic asymmetric unit consists of four monomeric units.

FACTORS GOVERNING THE STABLE MOLECULAR AND CRYSTAL STRUCTURE OF A POLYMER

In the course of X-ray structure analyses and normal coordinate treatment of various polymers we were interested in examining the factors which govern the stable crystal structure and molecular conformation of a polymer. *Figure 12* shows a molecular conformation of *isotactic* polypropylene, which has a (3/1) helical structure[35]. Here the conformational stability of such isotactic polymer chains is discussed based on energy calculations[36].

The *isotactic* polymers analysed were polypropylene, poly(4-methyl pentene-1), poly(3-methyl butene-1), and polyacetaldehyde. The X-ray analyses by Natta, Corradini *et al.* clarified the conformations of these polymers as (3/1)[35], (7/2)[37,38], (4/1)[39], and (4/1)[40], respectively. The conformational energies were calculated by taking into account the internal rotation barriers and the van der Waals and electrostatic interactions. We made the calculation without fixing the fibre identity period and only using the assumption that the chain forms a helical structure, i.e., the set of internal rotation angles repeats regularly along the subsequent monomeric units of the chain. The numbering of the internal rotation angles are given in *Table 1*[36]. The set of internal rotation angles for *isotactic* polypropylene and polyacetaldehyde is the simplest; τ_1 and τ_2. The others have additional rotation angles of the side chains, τ_3 and τ_4.

The potential map for polyacetaldehyde plotted against τ_1 and τ_2 is shown in *Figure 13* as an example[36]. There are two minimal points shown by crosses with the same potential value, corresponding to the right-handed and left-handed helices. The most stable conformation thus obtained agrees well with the actual X-ray analysed conformation shown by closed circles[40]. In *Table 2* are listed the internal rotation angles of the main chain τ_1 and τ_2 and the number of monomeric units per turn N for the

calculated stable conformations in comparison with the values for the actual conformations determined by X-ray analyses. The N values are in excellent agreements with the X-ray values in spite of the assumption of considering only the intramolecular interactions. This fact indicates that the molecular conformations of these *isotactic* polymers are mainly governed by the intramolecular interactions, especially by the steric hindrance of side chains. It is noteworthy, however, that in some cases the intermolecular interactions also may become an important factor determining the molecular conformations, as discussed later for poly(ethylene oxybenzoate) α form.

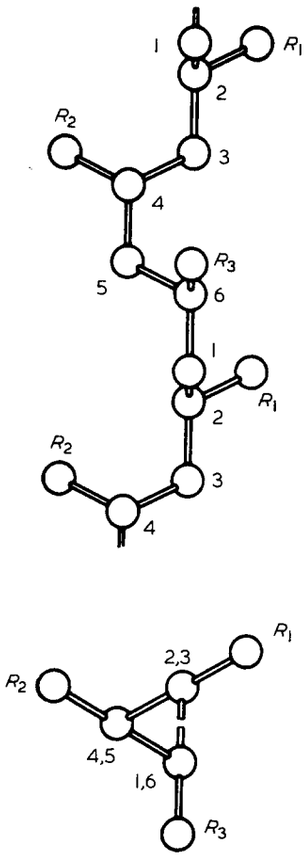

Figure 12 Molecular conformation of *isotactic* polypropylene[35]

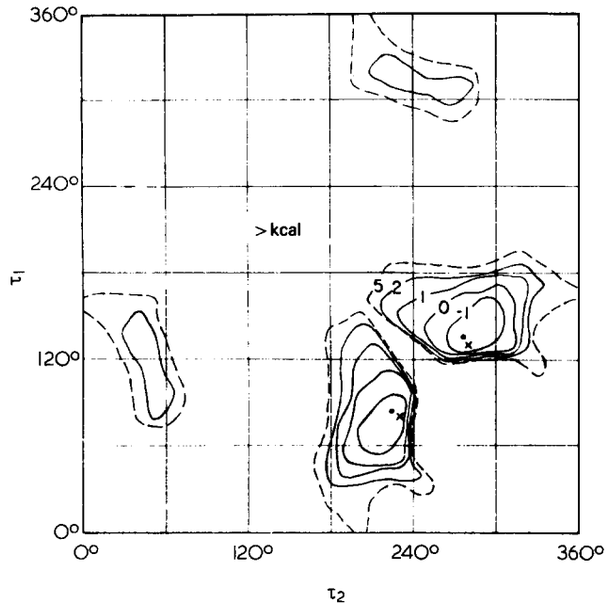

Figure 13 Potential energy map for *isotactic* polyacetaldehyde[36]

Table 2 Comparison of stable conformations obtained by energy calculations with those by X-ray structure analyses[36]

	Energy calculation[b]			X-ray work[c]		
Polymer[a]	τ_1	τ_2	N	τ_1	τ_2	N
it–PP	179°	–56°	2.91	180°	–60°	3.0
it–P4MP	155°	–68°	3.47	162°	–71°	3.5
it–P3MB	132°	–83°	4.17	149°	–81°	4.0
it–PAA	131°	–80°	3.94	136°	–83°	4.0

[a] *it*–PP: *isotactic* polypropylene, *it*–P4MP: *isotactic* poly(4-methyl pentene-1), *it*–P3MB: *isotactic* poly(3-methyl butene-1), *it*–PAA: *isotactic* polyacetaldehyde
[b] Torsional angles τ_1 and τ_2 are defined in *Table 1*
[c] *it*–PP, ref. 35; *it*–P4MP, ref. 37; *it*–P3MB, ref. 39; *it*–PAA, ref. 40

Table 1 Definition of internal rotation angles[36]

Polymer	Numbering	τ_1	τ_2	τ_3	τ_4
Polypropylene	$-C'_1H-C'_2MH-C_1H-C_2MH-C''_1H-$	$C'_1C'_2C_1C_1$	$C'_2C_1C_2$		
Poly(4-methyl pentene-1)	$-C'_1H-C'_2H-C_1H_1-C_2H_2-C''_1H-$ with τ_3 C_3H_3, τ_4 C_4H_4M	$C'_1C'_2C_1C_2$	$C'_2C_1C_2C''_1$	$H_2C_2C_3C_4$	$C_2C_3C_4H_4$
Poly(3-methyl butene-1)	$-C'_1H-C'_2H-C_1H_1-C_2H_2-C''_1H-$ with τ_3 C_3H_3M	$C'_1C'_2C_1C_2$	$C'_2C_1C_2C''_1$	$H_2C_2C_3H_3$	
Polyacetaldehyde	$-O'-C'MH-O-CMH-O''-$	O'C'OC	C'OCO''		

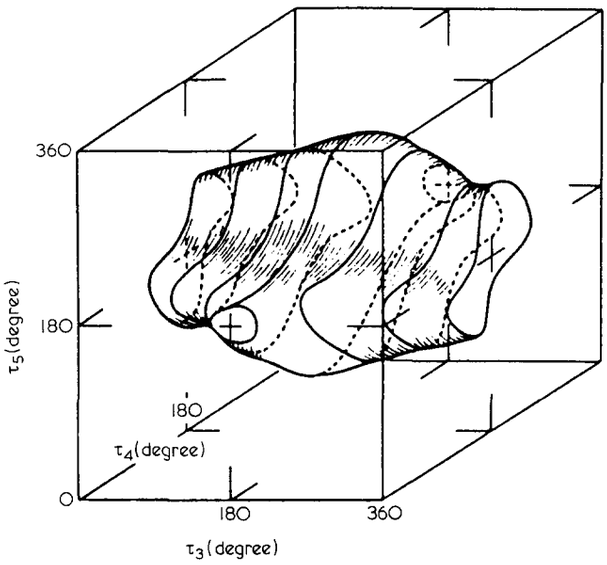

Figure 14 Three-dimensional closed surface for possible conformations of PEOB α form in the case of (2/1) helix with the fibre period 15.60 Å [41]

ORGANIZED COMBINATION OF METHODS OF X-RAY DIFFRACTION AND ENERGY CALCULATIONS FOR THE STRUCTURE ANALYSES OF IMPORTANT BUT COMPLICATED POLYMERS

Poly(ethylene oxybenzoate) α form[41]

The chemical structure of poly(ethylene oxybenzoate) (PEOB) corresponds to the structure of poly(ethylene terephthalate) (PET) with one carbonyl group removed; a lower symmetry structure:

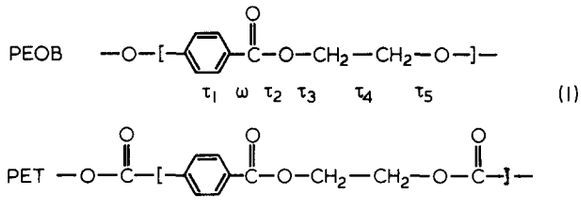

As indicated in equation (1), PEOB has a large number of freedom of the internal rotation of the bonds; τ_1 for the virtual bond (O–benzene–C), ω the dihedral angle between the planes of the benzene ring and the ester group, τ_2, τ_3, τ_4, and τ_5. First we examined the internal rotation angles except for ω by assuming that the angle τ_2 of the ester group is essentially 180° and that the fibre period is 15.60 Å. As shown in *Figure 14*, the possible conformations are limited on the closed surface in the cube defined by the three-dimensional Cartesian coordinates τ_3, τ_4, and τ_5. If τ_3 and τ_4 are given, τ_5 should take two values, upper and lower intersecting points of the surface, resulting also in the generation of a pair of values of τ_1. Furthermore, the dihedral angle ω should be considered also. We calculated the intramolecular potential energy for ≈ 5000 models thus obtained. From the results the seven stable molecular models are chosen, among which only one model gives reasonably good agreement between the observed and calculated X-ray diffraction intensities. Although we refined this model by repeating trial-and-error procedures by utilizing the constrained least-squares method, this model did not converge to the final structure with a reasonable discrepancy factor.

Then we considered that the intermolecular interaction may be important, so the newly derived packing energy minimization method was applied, and eventually the final structure was established. The internal rotation angles of the initial model and the final structure are given in *Figure 15* together with their differences. The differences in τ_1, ω, and τ_3 are especially large, 25°–28°. The rotation angle ω changed from 10° to −15°, corresponding to a large rotation of the benzene plane. This example exhibits both the usefulness and limitation of intramolecular interaction energy calculation as the method to obtain the molecular models suitable for structure analyses; the initial model was obtained through the calculation of the intramolecular interaction energy, but the final model could not be obtained without the application of packing energy minimization. *Figure 16* shows the crystal structure thus determined. The molecular chain

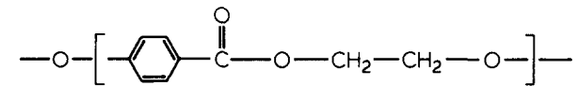

	τ_1	ω	τ_2	τ_3	τ_4	τ_5
Initial	-41°	10°	-180°	-75°	-60°	-164°
Final	-13°	-15°	-172°	-102°	-59°	-186°
Difference	28°	25°	8°	27°	1°	22°

Figure 15 Conformational angles of PEOB α form for initial and final models and their differences[41]

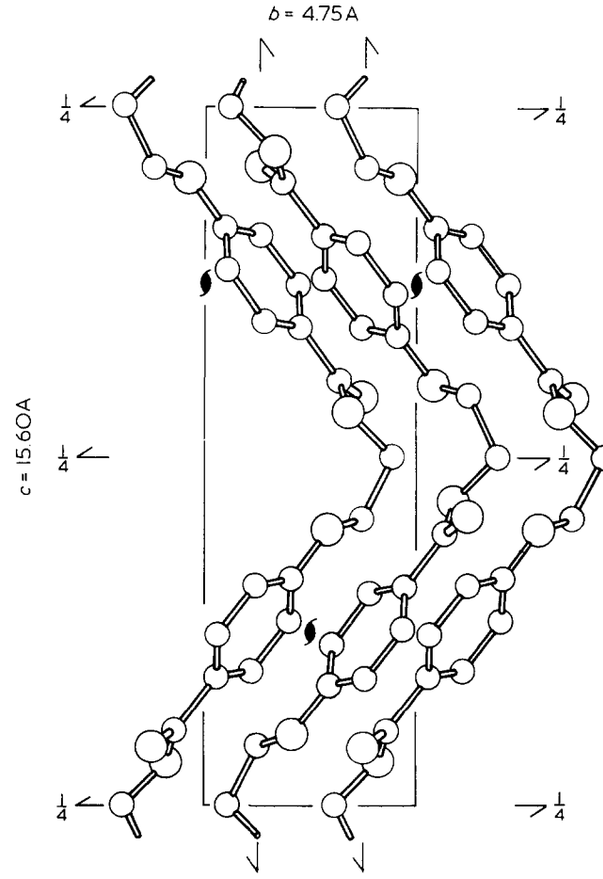

Figure 16 Crystal structure of PEOB α form[41]

has a zig-zag conformation of large scale, one monomeric unit being a zig-zag unit. This unique structure can be related to the unusually low crystallite modulus, a problem which is discussed later.

Isotactic *poly(methyl methacrylate)*

The structure of *isotactic* poly(methyl methacrylate) (*it* PMMA) had not long been determined. For this polymer, models of (5/2) and (5/1) helices had been proposed[42,43]. We started the analysis in 1966, and after a long roundabout quest we determined the crystal structure which consists of double strand helices in 1976[44]. During the analysis in 1970, we considered the (5/1) helix to be most reasonable at that stage[45]. Thereafter we made efforts of trial-and-error for obtaining the crystal structure model but no reasonable packing was found for the (5/1) helices in the orthorhombic lattice of $a = 20.98$ Å, $b = 12.06$ Å, and c (fibre axis) $= 10.40$ Å. However, the calculation of the intramolecular interaction energy suggested that the helices with larger radii such as a (12/1) helix should be more stable than the (5/1) helix[36]. *Figure 17* shows the potential energy counter map. The lowest minimum was found at the position corresponding to a (12/1) helix. The minimum corresponding to the (5/1) helix has a higher energy value, the difference being ≈ 13 kJ mol^{-1} of monomeric unit.

By taking into account these facts, we re-examined the molecular models with larger radii, and found that the X-ray data can be explained satisfactorily by the crystal structure consisting of double helices as shown in *Figure 18*, the first case for synthetic polymers[44]. The double helix consists of two chains denoted by solid and broken lines shifting 10.40 Å along the helix axis of each other, and gives the fibre identity period of 10.40 Å, coinciding with the observed value. Each chain has ten monomeric units and one turn in the period of 20.80 Å, i.e., (10/1) helix. The molecular parameters assumed for (10/1) helix are as follows; (1) the bond lengths and bond angles are the same as for the previous (5/1) helix model[45] except for $\angle C\text{–}CH_2\text{–}C = 124°$, (2) the α-CH_3 group points outward, and (3) $\tau_1 = -179°$, $\tau_2 = -148°$, $\tau_3[MCC(O)O] = -24°$, and $\tau_4[CC(O)OM] = 174°$ (*cf.* Fischer projection, equation (2)) for a right-handed helix with the ester group pointing upward as shown in *Figure 18*.

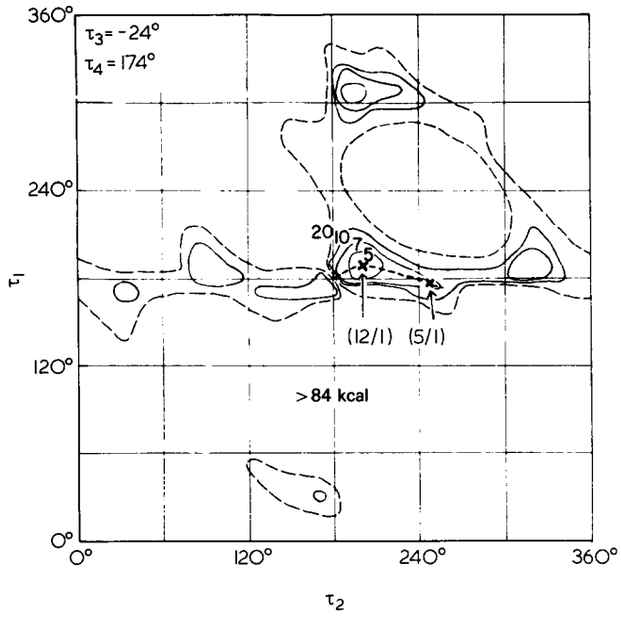

Figure 17 Potential energy map for *it* PMMA chain[36]

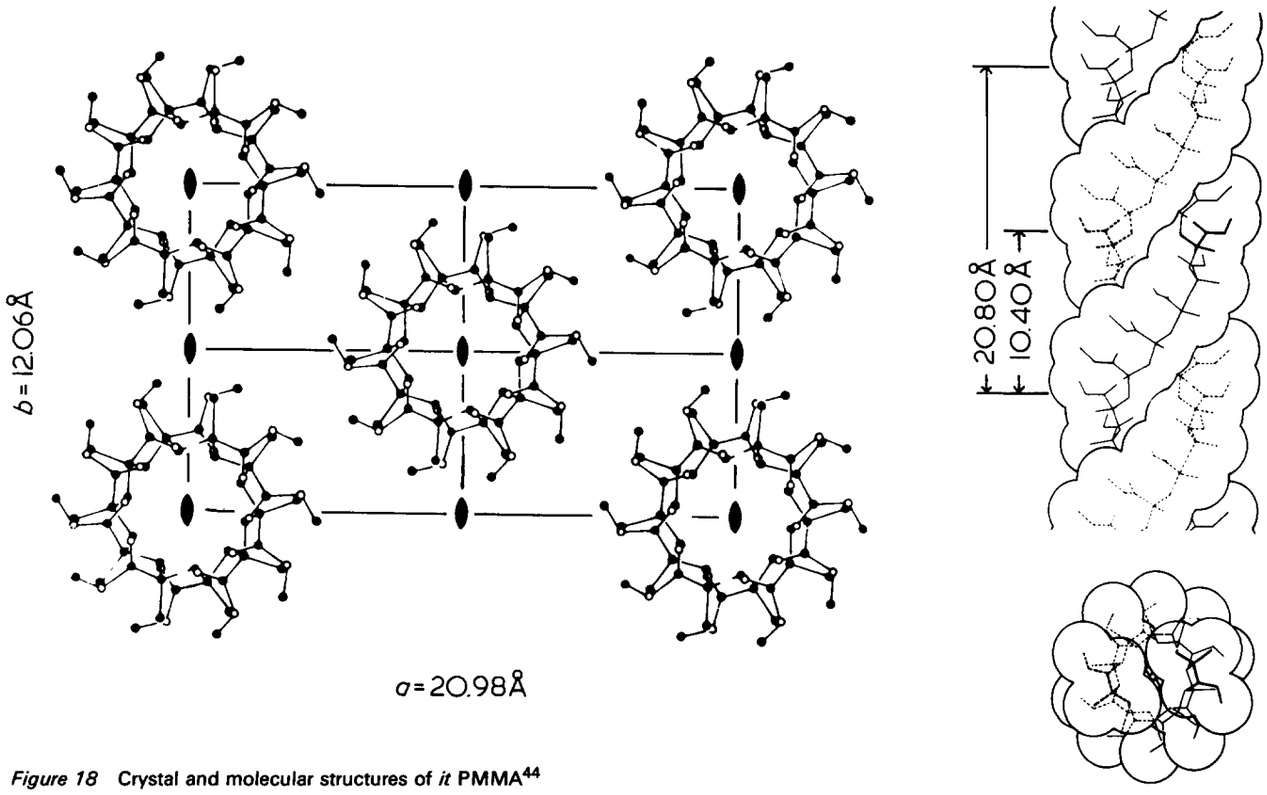

Figure 18 Crystal and molecular structures of *it* PMMA[44]

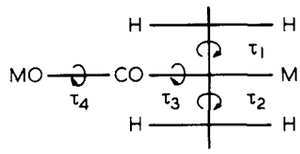

(2)

The result of energy calculations also indicated that the double helix is 18.4 kJ mol^{-1} of monomeric unit more stable than two isolated (10/1) helices. This result suggests the stabilization is due to good fitting of the intertwined two chains, although there is no hydrogen bonding between them as in the case of DNA. Further refinement of the crystal structure consisting of double helices is now difficult, because the X-ray photograph is not as well defined, and the possibility of disordered structure is also considered, which consists of statistical packing of right- and left-handed helices with upward and downward pointing ester groups. However, the present structure is not merely a proposal of a new model, but is believed to be essentially correct.

Polyethylene imine

Polyethylene imine [–(–CH_2–CH_2–NH–)–, PEI] forms three types of hydrates (CH_2CH_2NH:H_2O = 0.5, 1.5, and 2)[46-48]. The molecular conformation of hydrates are planar zig-zag but the anhydrate forms a double helix as shown in *Figure 19*, the second one found for synthetic polymers[48]. One chain is a (5/1) helix with the identity period 9.48 Å and two chains with the same sense of helix intertwine by rotating 180°. The important factor of double helix formation is intermolecular hydrogen bonds N–H...N (3.18 Å).

Syndiotactic *poly(methyl methacrylate)*

In connection with *it* PMMA, *syndiotactic* poly(methyl methacrylate) (*st* PMMA) is also an interesting polymer. This polymer is difficult to crystallize on thermal treatment, but we have succeeded in preparing the oriented crystalline sample by absorption of such solvents as chloroacetone into the stretched non-crystalline sample (solvent-induced crystallization)[49]. The X-ray structure analysis revealed that *st* PMMA forms non-stoichiometric inclusion compounds with a variety of solvents[50]. *Figure 20a* shows a schematic illustration of the crystal structure of *st* PMMA–solvent complexes. Because of the steric hindrance between the bulky side groups of adjacent monomeric units, *st* PMMA chains take a helical structure which has a sufficiently large radius as shown in *Figure 20b*. Hence, the solvent molecules are included in the cavities of inner- and inter-helices. The solvent molecules may be indispensable to stabilize the large helical conformation, being the reason why *st* PMMA can crystallize only by solvent treatment and why the crystallinity is lost by desorption of solvent.

STRUCTURE AND OPTICAL COMPENSATION OF OPTICALLY ACTIVE POLYMERS

Isotactic poly(*tert*-butylethylene oxide) (*it* PtBEO) has a truely assymetric carbon atom in each monomeric unit, giving two types of optical isomers, rectus (R) and sinister (S) as shown in *Figure 21*. There exist three crystal modifications (I, II, and III) for this polymer and here modification I is discussed[51].

The general feature of the X-ray data suggests that a large tetragonal unit cell contains four chains with (9/4) helical conformation. Coupling the X-ray structure analysis with potential energy calculation, we determined the crystal structure as shown in *Figure 22*. The molecules at the upper-left and lower-right positions in this Figure are right-handed helices of sinister optical isomer, and those at the upper-right and lower-left positions are left-handed helices of rectus isomer. Although this Figure shows the upward helices only for simplicity, the actual structure is considered to be statistically disordered, consisting of upward and downward helices in 1:1 ratio. It may be an interesting fact that two pairs of optical antipodes pass through the definite positions of the unit cell, resulting in the racemic unit cell.

We have analysed the crystal structures of many optically active polymers such as *it* PtBEO[51], *isotactic* poly(propylene sulphide)[52], etc.[53-56]. The method of optical compensation of racemic polymers, which consist of equal amounts of optically antipodal chains, may be classified as shown in *Figure 23*. The *it* PtBEO modification I mentioned previously is an example of racemic lattice (a), where two pairs of optical antipodes are included in the lattice. As shown in *Table 3*, *isotactic* poly(*tert*-butylethylene sulphide) is also an example of racemic lattice[56]. *Figure 23b* shows optical compensation in a crystallite. Rectus and sinister polymers are packed irregularly in a crystallite with equal weights, that is, a statistically random structure. Intercrystallite compensation (c) is found for such polymers as *isotactic* poly(propylene sulphide)[52], *isotactic* poly-β-hydroxybutyrate[53], etc., where the racemic sample consists of crystallites, each composed only of rectus polymer

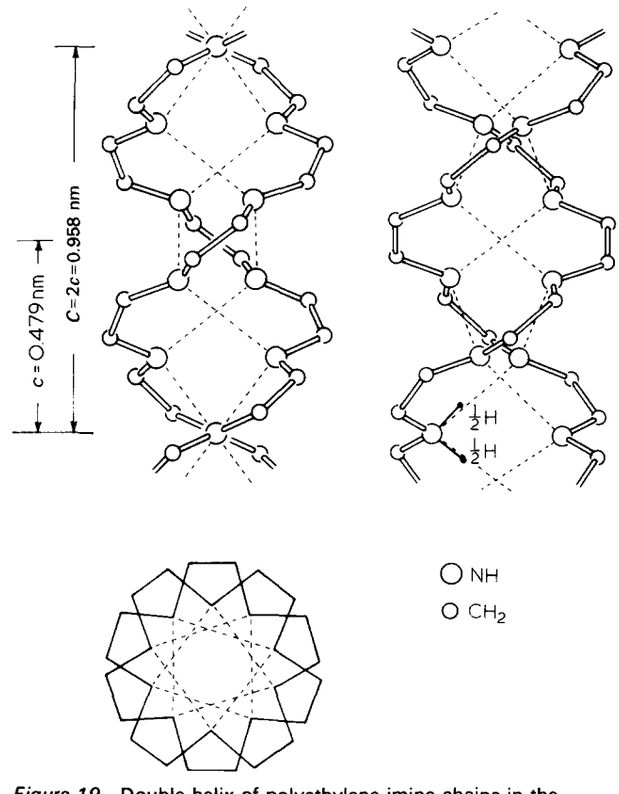

Figure 19 Double helix of polyethylene imine chains in the anhydrate.[47] Broken lines indicate NH...N hydrogen bonds

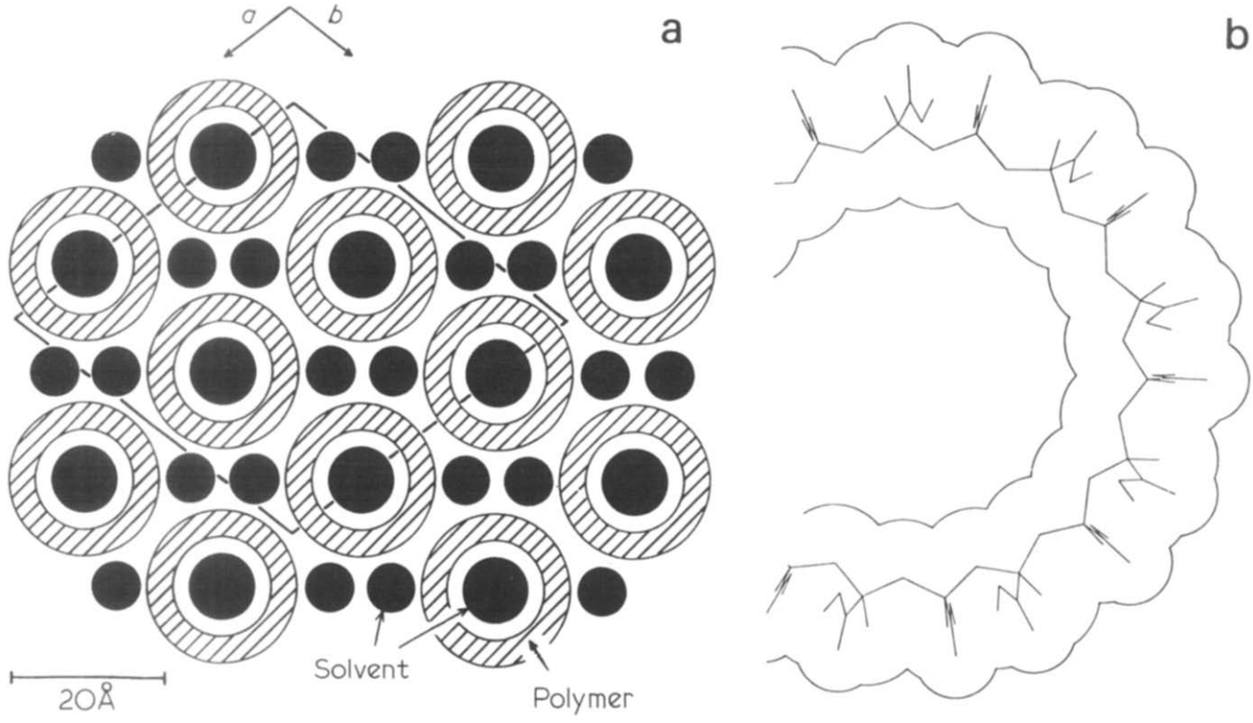

Figure 20 (a) Schematic illustration of *st* PMMA-solvent complex viewed along the fibre axis.[49,50] Hatched and shadow regions indicate the polymer chains and solvent molecules, respectively. (b) Helical structure of *st* PMMA chain in the complex

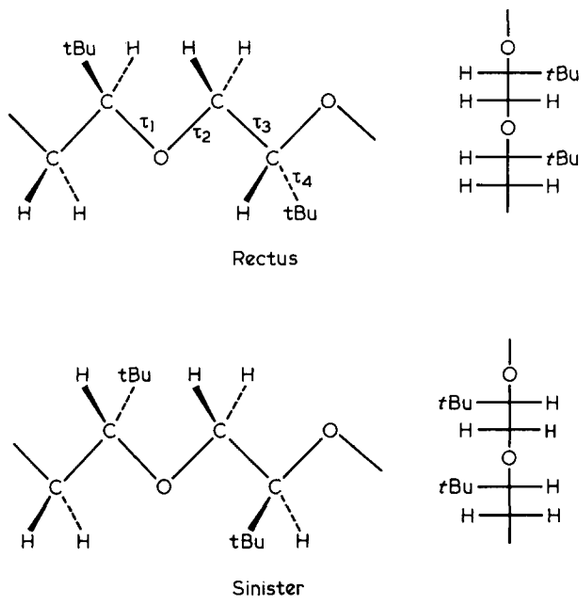

Figure 21 Absolute configuration of two types of optical isomers for *isotactic* poly(*tert*-butylethylene oxide)[51]

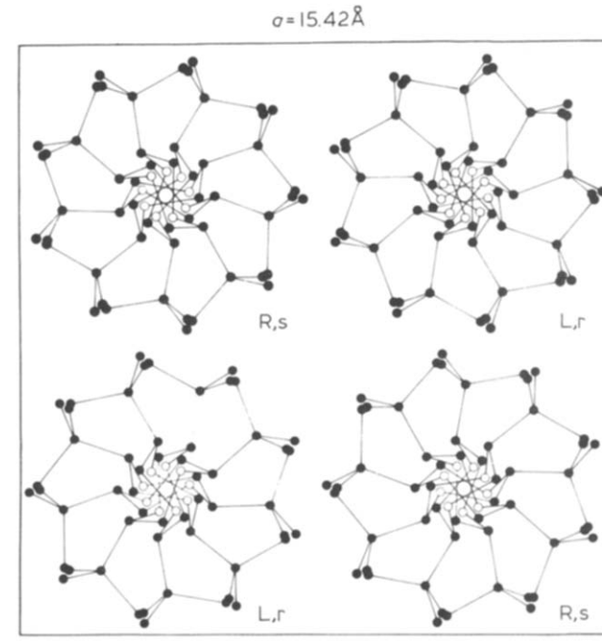

Figure 22 Crystal structure of *isotactic* poly(*tert*-butylethylene oxide) modification I.[51] Only the upward helices are illustrated for simplicity. R, rectus; S, sinister; r, right-handed; l, left-handed

chains or only of sinister polymer chains, and compensation by the same amounts of optical antipodes occurs.

RELATION BETWEEN STRUCTURE AND PROPERTIES

Crystallite modulus and molecular conformation

The crystallite modulus was first measured by Dulmage and Contois[57] by using an X-ray diffraction method for poly(ethylene terephthalate) based on the assumption of a mechanical series model. In the series model it is assumed that the molecular chains pass through the crystalline and amorphous regions along the fibre axis, so that the crystalline and amorphous regions are subjected to the same magnitude of stress[58]. Two other types of method of measurement have been invented: one uses the longitudinal acoustic mode (LAM) appearing in Raman spectra[59], and the other is based on the frequency-phase relation curves obtained from the neutron coherent

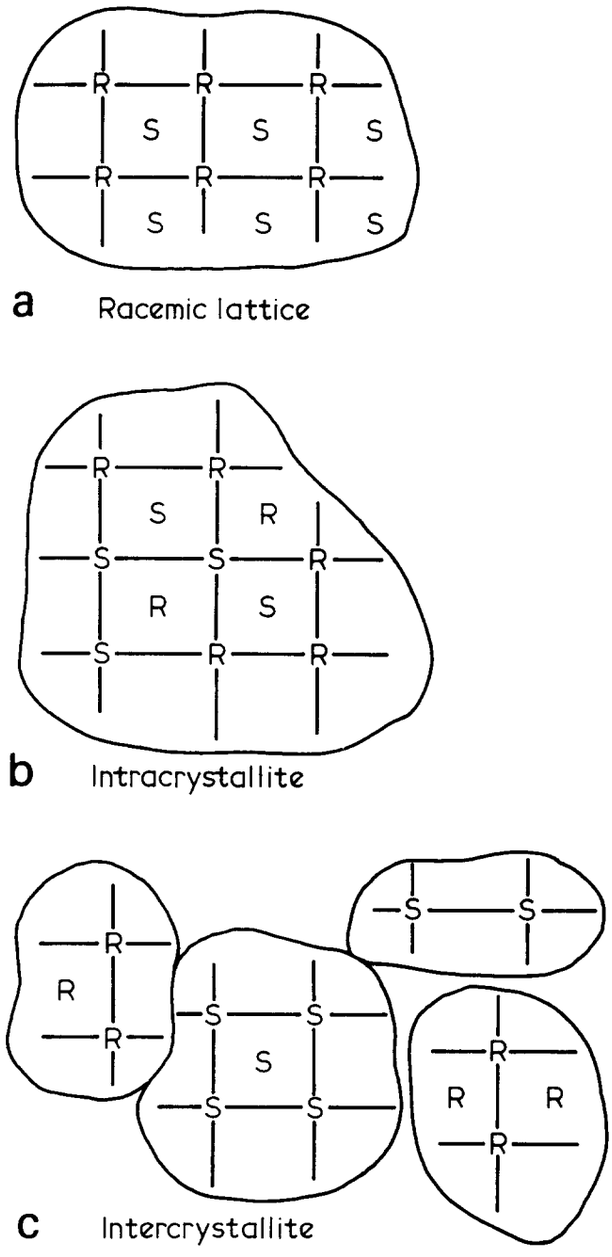

Figure 23 Method of optical compensation of racemic polymers. (a) Compensation in a unit cell; (b) compensation in a crystallite; (c) intercrystallite compensation. R and S show rectus and sinister polymer chains, respectively[51]

inelastic scattering[60]. The crystallite modulus can be calculated theoretically[61-64]; the geometrical structure should utilize the X-ray analysed one, and the force constants are supplied from the vibrational analyses of infrared and Raman spectra.

As an example, poly-*p*-phenylene terephthalamide (Kevlar or Fiber B) is discussed here[65]. Kevlar has high tenacity and high modulus, and is stable up to high temperature.

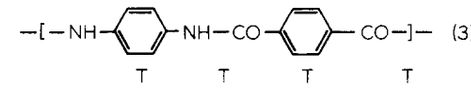

These characteristic features can be reasonably interpreted by the results of structure analysis. The crystal structure determined in our laboratory[66] and independently by Northolt in Holland[67] is shown in *Figure 24*. The molecular conformation is fully extended all *trans*, TTTT, as shown in equation (3). These *trans* chains form hydrogen-bonds (indicated by broken lines) in the *bc* plane and the sheets composed of such hydrogen-bonded chains stack along the *a* axis.

Macroscopic and crystallite moduli are listed in *Table 4* for various fibres[65]. For Kevlar the macroscopic modulus is 111 GPa, very high compared with the usual fibres. The crystallite modulus of Kevlar calculated based on the crystal structure is 182 GPa, which agrees with the observed X-ray values 153[68] and 200 GPa[69]. Because Kevlar has all *trans* molecular conformation, the changes in internal rotational angles cannot contribute to the elongation of the molecular chain. The elongation can arise only from the changes of the bond angles and bond lengths. *Figure 25* shows schematically the calculated displacements of the atoms by assuming hypothetically large elongation of 10% for Kevlar molecule[65]. The solid lines denote the positions before elongation and dashed lines after elongation. The deformation should occur so as to minimize the potential energy as a whole. The distribution of the potential energy of strain to the internal coordinates can be calculated based on this principle. In the Figure some of those with large values are shown as a percentage. In Kevlar, 23% of the energy distributes to the deformation of the bond angles ∠ benzene–C(O)–N.

Figure 26 shows the calculated atomic displacements for polyethylene (PE), an example of the largest crystallite modulus, poly(ethylene oxybenzoate) (PEOB) α form, the smallest crystallite modulus, and poly(ethylene terephthalate) (PET), the intermediate one[65]. In PE the potential

Table 3 Optical compensation of several *isotactic* polymers

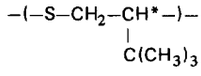	Racemic lattice[56]	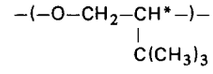	Racemic lattice (form I)[51] Intercrystallite (form II)[a]
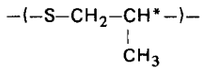	Intercrystallite[52]	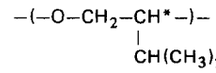	Intercrystallite[55]
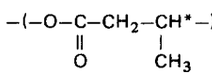	Intercrystallite[53]	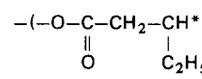	Intercrystallite[54]

[a] The method of optical compensation of poly(*tert*-butylethylene oxide) form III has not yet been clarified

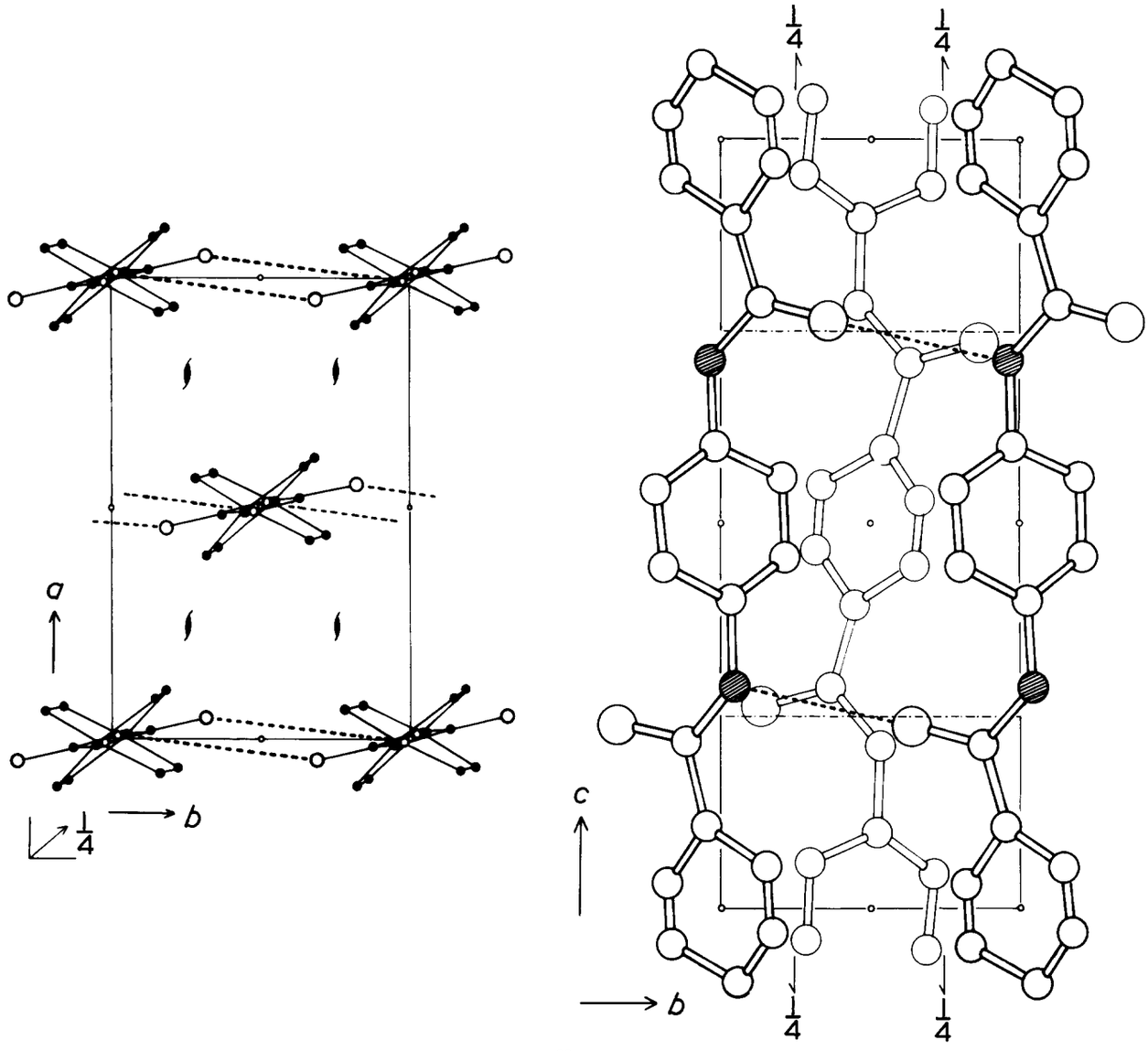

Figure 24 Crystal structure of poly-*p*-phenylene terephthalamide.[66] Broken lines show NH...O hydrogen bonds

Table 4 Young's moduli for various polymers[65]

Polymer[a]	Macroscopic modulus (GPa)	Crystallite modulus (GPa)	
		Obsd.	Calcd.
Kevlar	111	153 200	182
PRD–49	134	–	163
it–PP	10	34	40
Nomex	10	88	90
PET	20	108	95
Nylon 6 (α)	5	165	244
PE	9	235	316
PEOB (α)	9	6	2

[a] PRD–49, poly-*p*-benzamide; Nomex, poly-*m*-phenylene isophthalamide. Abbreviated names of other polymers are referred to in the text

energy distribution is 53% to the bond stretching, and 47% to the bond angle bending. This is a special case in which the contribution of the bond stretching is large. PEOB α form is another extreme case, having very low crystallite modulus 6 GPa. The low crystallite modulus can be understood from the crystal structure. As stated previously, the conformation of PEOB α form is a large scale zig-zag, one monomeric unit being a zig-zag unit[41]. The deformation of the large zig-zag occurs mainly due to the internal rotation of the bonds, as seen from the potential energy distributions. Because of these two factors, i.e., the long length (≈ 6 Å compared with 0.9 Å in PE) of the arm or the component of the moment of force, and the small values of the internal rotation force constants, the crystallite modulus of PEOB α form is very small.

Three-dimensional crystallite modulus

Theoretical calculation of three-dimensional elastic constants is desirable for further understanding of mechanical behaviour of crystalline polymers. Such calculations have been carried out by several researchers[70–72]. However, these methods require the parameters concerning all atoms in one unit cell and, therefore, need a large computer time. Thus, the application of the methods has been restricted, so far, to the simplest case of orthorhom-

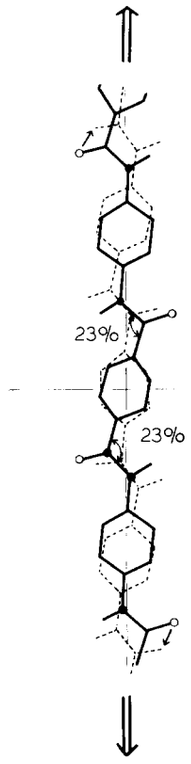

Figure 25 Atomic displacements and potential energy distributions for Kevlar chain when the chain is stretched 10% [65]

bic PE. We derived a method which can start from parameters for a crystallographic asymmetric unit by taking into account the space group symmetry[73]. The asymmetric unit is the smallest unit related to others by symmetry operations. For PE the asymmetric unit is one methylene group and the number of the starting parameters can be reduced to one-fourth, as one unit cell contains four methylene groups. Hence, the calculation has become easier for more complicated structures.

Utilizing the defined structure parameters[74] and the suitable potential functions[75] which can reproduce well the vibrational frequencies, heat capacity, etc., the elastic and compliance constants of orthorhombic PE crystal are calculated as follows at room temperature[76]:

Elastic constants

$$C = \begin{bmatrix} 7.99 & 3.28 & 1.13 & & & 0 \\ 3.28 & 9.92 & 2.14 & & & \\ 1.13 & 2.14 & 315.92 & & & \\ & & & 3.19 & & \\ & & & & 1.62 & \\ 0 & & & & & 3.62 \end{bmatrix} \text{GPa}$$

Compliance constants

$$S = \begin{bmatrix} 14.48 & -4.78 & -0.02 & & 0 & \\ -4.78 & 11.67 & -0.06 & & & \\ -0.02 & -0.06 & 0.32 & & & \\ & & & 31.31 & & \\ & & & & 61.86 & \\ 0 & & & & & 27.60 \end{bmatrix} \times 10^{-2} \text{ (GPa)}^{-1}$$

Figure 27 shows the anisotropy of Young's modulus in the *ab* plane of orthorhombic PE crystal. The magnitude of the modulus is shown by the distance between the centre of the unit cell and a particular point on the curve in this direction. The solid curve is drawn to fit the values observed by Sakurada *et al.*[77], indicated by bars, where the series model is assumed in all directions in the *ab* plane. The broken curve is the theoretical value and is of the same order as the experimental curve. *Figure 28* shows the linear compressibility for orthorhombic PE crystal. The agreement between the calculated curve (broken line) and the experimental result obtained by Ito[78] (solid curve) is excellent. The linear compressibility is measured by X-ray diffraction under hydrostatic pressure without any assumption of stress distribution within the sample and, therefore, is highly reliable.

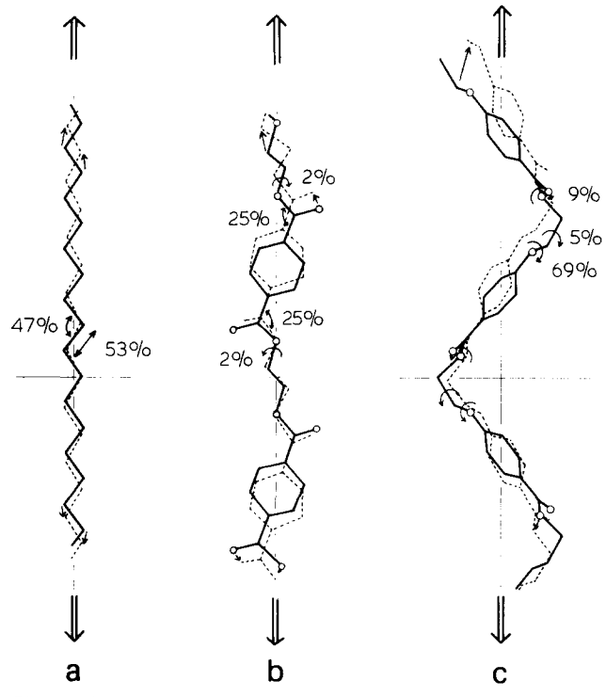

Figure 26 Atomic displacements and potential energy distributions for (a) polyethylene; (b) poly(ethylene terephthalate); and (c) poly(ethylene oxybenzoate) α form when the chains are stretched 10% [65]

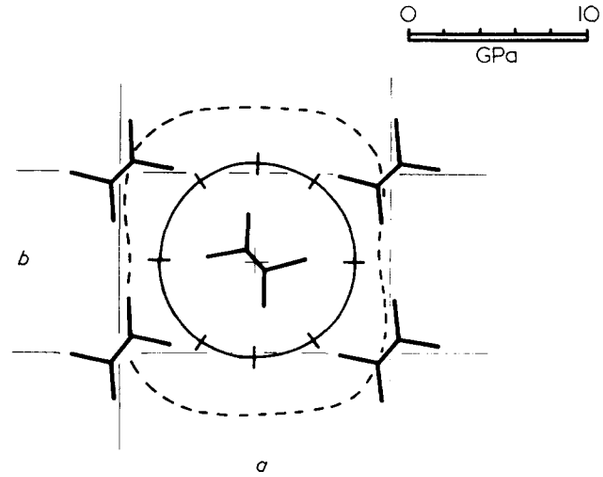

Figure 27 Anisotropy of Young's modulus in the *ab* plane of orthorhombic polyethylene crystal. ——, observed by Sakurada *et al.*;[77] – – –, calculated by Tadokoro *et al.*[76]

We have calculated the elastic and compliance matrices for various types of polymer crystals such as *atactic* poly(vinyl alcohol) (PVA)[76], poly(vinylidene fluoride)[79], nylon 6 α and γ forms[80], *isotactic* polypropylene[81], etc. and obtained a good agreement between the observed and calculated values. *Table 5* shows the calculated crystallite moduli in the chain direction of the four polymers with and without taking into consideration the intermolecular interactions[80]. The influence of intermolecular interactions is hardly detected for planar-zig-zag PE, PVA, and nylon 6 α form because the crystallite modulus along the chain direction is almost determined by the bond stretching and the bond angle deformation of the skeletal linkages, as stated previously. The modulus of the γ form of nylon 6, in contrast, is affected largely by intermolecular interactions. In this case the molecular chain is contracted from the zig-zag form, and the potential energy of strain distributes mainly to the torsional deformations of the CH_2-amide bonds. Such torsional deformations are, in general, influenced greatly by the intermolecular interactions because of the small force constants of the internal rotations, comparable to those of intermolecular interactions.

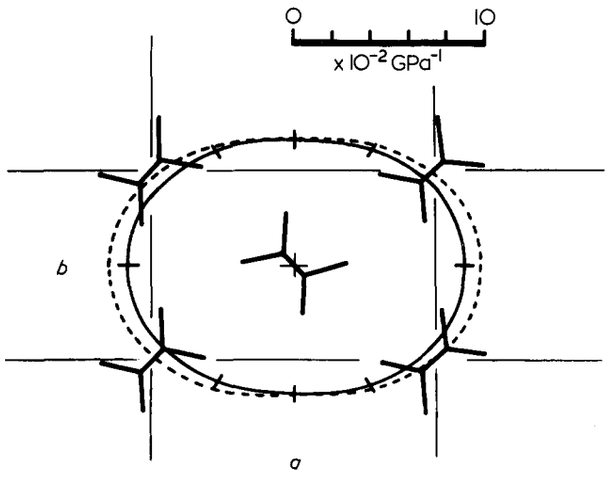

Figure 28 Anisotropy of linear compressibility of orthorhombic polyethylene crystal. ———, observed by Ito *et al.*;[78] – – –, calculated by Tadokoro *et al.*[76]

Piezoelectricity of poly(vinylidene fluoride)

Since 1971, we have found many crystalline modifications of poly(vinylidene fluoride) (PVDF) and determined their crystal structures, as shown in *Figure 29*[82,83], where a large circle represents a fluorine atom. The molecular chain of form I takes an essentially planar-sig-zag conformation. These chains are packed in the

Table 5 Influence of intermolecular interactions on the crystallite modulus along the chain direction (GPa)[a]

			Nylon 6	
	PE	PVA	α	γ
Calcd with all intermol interactions	315.5	287.4	311.5	53.7
Calcd without hydrogen bonds	–	287.4	311.5	51.8
Calcd without intermol interactions	315.4	287.2	288.6	24.9

[a] The detailed parameters used in calculations are referred to ref. 80

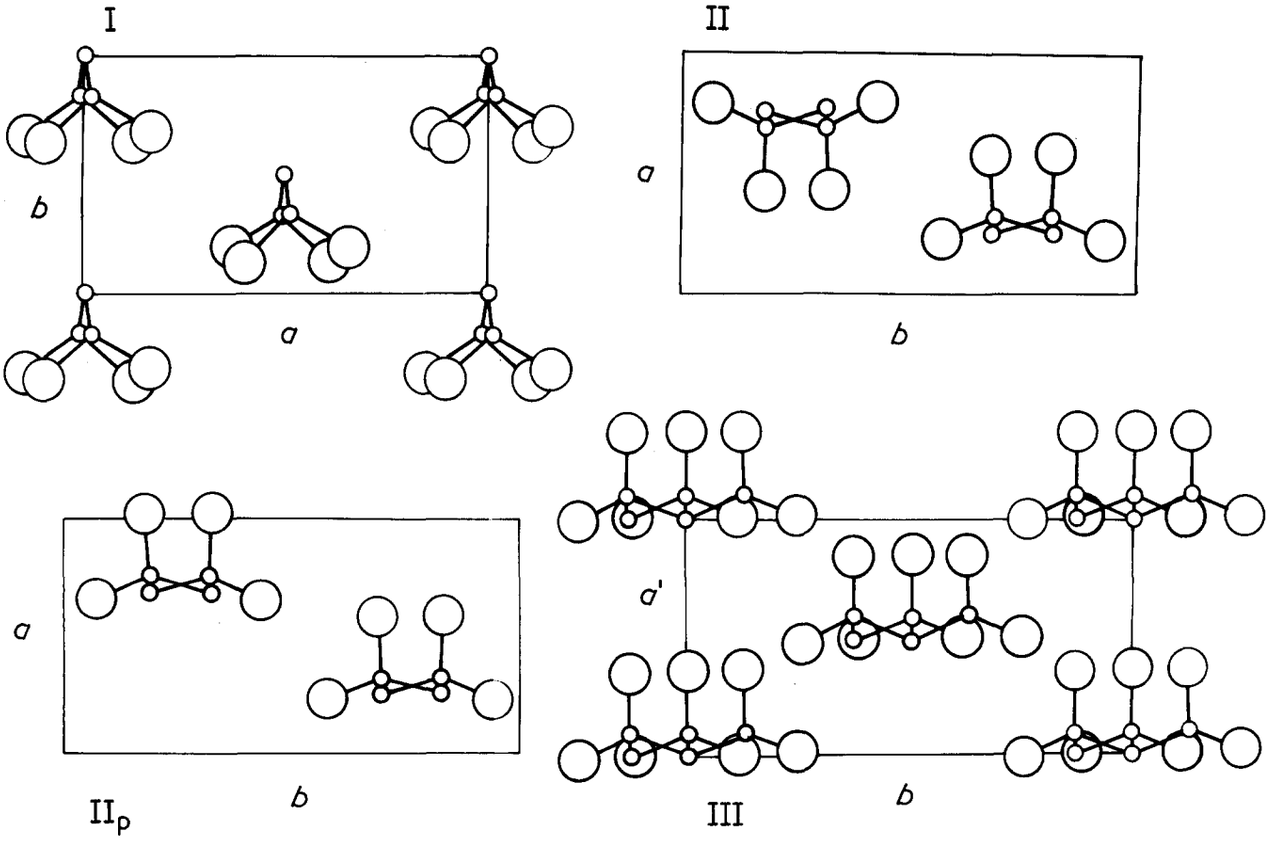

Figure 29 Crystal modifications of poly(vinylidene fluoride)[79]

Table 6 Percentages of contribution of various parameters to the macroscopic piezoelectric strain constants of PVDF Form I[a]

	κ^a	σ^m	ΔV^c	d^c
d_{31}^m	5.4%	87.9%	−6.6%	13.4%
d_{32}^m	−8.8	96.2	8.7	3.8
d_{33}^m	1.7	88.6	−7.9	17.6

[a] κ^a, electrostriction constant of the amorphous phase; σ^m, Poisson's ratio of the film; ΔV^c, volume compressibility of the crystal phase; d^c, intrinsic piezoelectric strain constants of the crystal phase. Details are referred to ref. 88

lattice so that the dipoles are parallel along the *b* axis. Therefore, the crystal is polar. Form II is non-polar and two TGTḠ conformational chains are connected to each other by point of symmetry. When form II is subjected to the high electric field, it transforms to polar form II, where the TGTḠ chains are arranged in parallel in the unit cell as reported by several groups[84,85]. In form III the $T_3GT_3\bar{G}$ chains are packed in parallel in the unit cell and so this is a polar structure. Among these crystalline modifications, form I exhibits the largest piezoelectric effect of all the synthetic piezoelectric polymers[86].

The piezoelectric effect is a phenomenon where an electric voltage is observed on the film surface when the film is tensioned along a certain direction. The magnitude of piezoelectric effect is represented by the piezoelectric constants (*d*, *e*). For example, when we measure the voltage in the 3rd axis direction induced by tension along the 1st axis, the piezoelectric strain constant d_{31}^m and stress constant e_{31}^m are detected, where the superscript m denotes the macroscopic value. In the case of PVDF form I film, the d_{31}^m is ≈ 20 pC/N at room temperature, similar to the value 25 pC/N of triglycine sulphate. The reason why such a large piezoelectric effect can be observed for this polymer was for a long time unclear. We tried to solve this problem from the structural point of view[79,87,88].

We calculated the piezoelectric constants of PVDF form I crystal based on the lattice dynamics. The calculated d_{31}^c of crystal is ≈ -0.25 pC/N and d_{33}^c is ≈ -25 pC/N, which are in good agreement with the values observed by Odajima *et al.*[89]. But the macroscopic d_{31}^m value is ≈ 20 pC/N, 2 orders higher than the crystalline d_{31}^c value. Therefore, we can not explain simply the macroscopic piezoelectric effect in terms of the intrinsic piezoelectricity of the crystal phase alone. Then we considered the coupling effect of the polar crystalline phase and the nonpolar amorphous phase. Based on this coupling model, the macroscopic piezoelectric constant d_{3i}^m can be expressed in terms of several physical parameters such as dielectric constant ε^a and electrostriction constant κ^a of the amorphous phase, Poisson's ratio σ^m of the film, volume compressibility ΔV^c and intrinsic piezoelectric constants d^c of the crystal phase, etc. Based on these equations we calculated the macroscopic piezoelectric constants of PVDF form I film as follows:

$$d_{31}^m = 25.3 \text{ pC/N}, \; d_{32}^m = 7.0 \text{ pC/N}, \; d_{33}^m = -35.4 \text{ pC/N}$$
at room temperature.

These are in good agreement with the observed values ($d_{31}^m \approx 20$ pC/N, $d_{32}^m \approx 2$ pC/N, $d_{33}^m \approx -30$ pC/N), indicating that the coupling model of crystalline and amorphous phases is reasonable. *Table 6* shows the percentage contribution of the various factors affecting the macroscopic piezoelectric constants, where the minus sign means a negative contribution reducing the piezoelectric effect. Of these factors the intrinsic piezoelectric effect of crystal lattice d^c contributes $\approx 15\%$, and the largest contributor is Poisson's ratio σ^m, $\approx 90\%$. In conclusion it appears that the film exhibiting the larger change in thickness induced by tensile strain has a possibility to show the higher piezoelectric effect. Also, such an idea has been proved experimentally[79,87,88].

Stability of crystal forms of polyethylene and vibrational free energy

Polyethylene has two crystal forms as shown in *Figure 30*: the stable orthorhombic form[90] and the metastable monoclinic form[91]. According to the results of static potential energy calculations by Yemni and McCullough[92], the monoclinic form is more stable by ≈ 0.15 kJ mol^{-1} of the methylene unit than the orthorhombic form, opposed to the experimental finding. In a discussion of such crystal stability, the vibrational free energy is an important factor.

To calculate the free energy[93], the frequency distribution must be obtained by using the force constants assumed based on the infrared and Raman spectra. *Figure 31* shows the calculated frequency distribution curves in the region <600 cm^{-1} for the two forms of PE. The difference between the two forms is marked in the region <200 cm^{-1}. The orthorhombic form exhibits the frequency distribution toward the lower frequency side, reflecting on the larger entropy of the orthorhombic form.

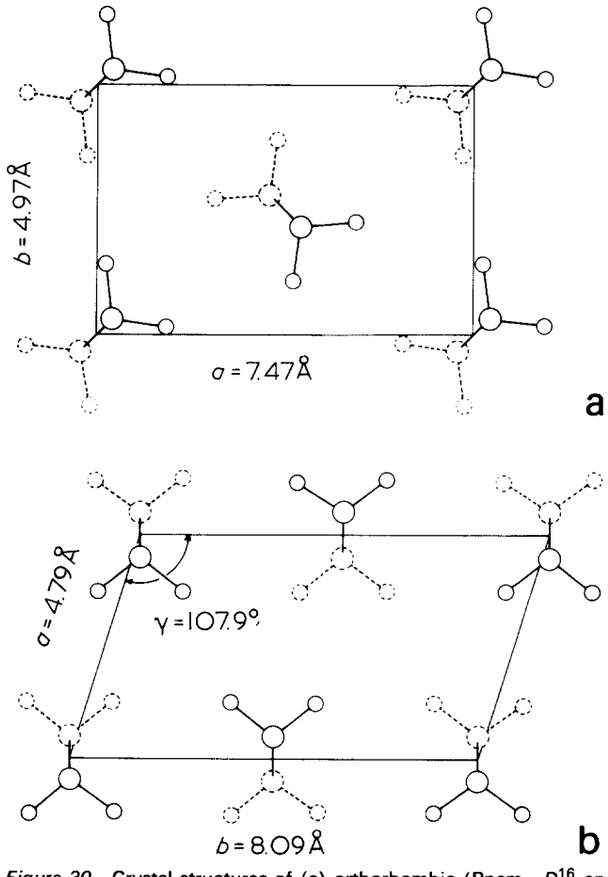

Figure 30 Crystal structures of (a) orthorhombic (Pnam – D_{2h}^{16} and (b) monoclinic ($A2/m - C_{2h}^3$) polyethylene[93]

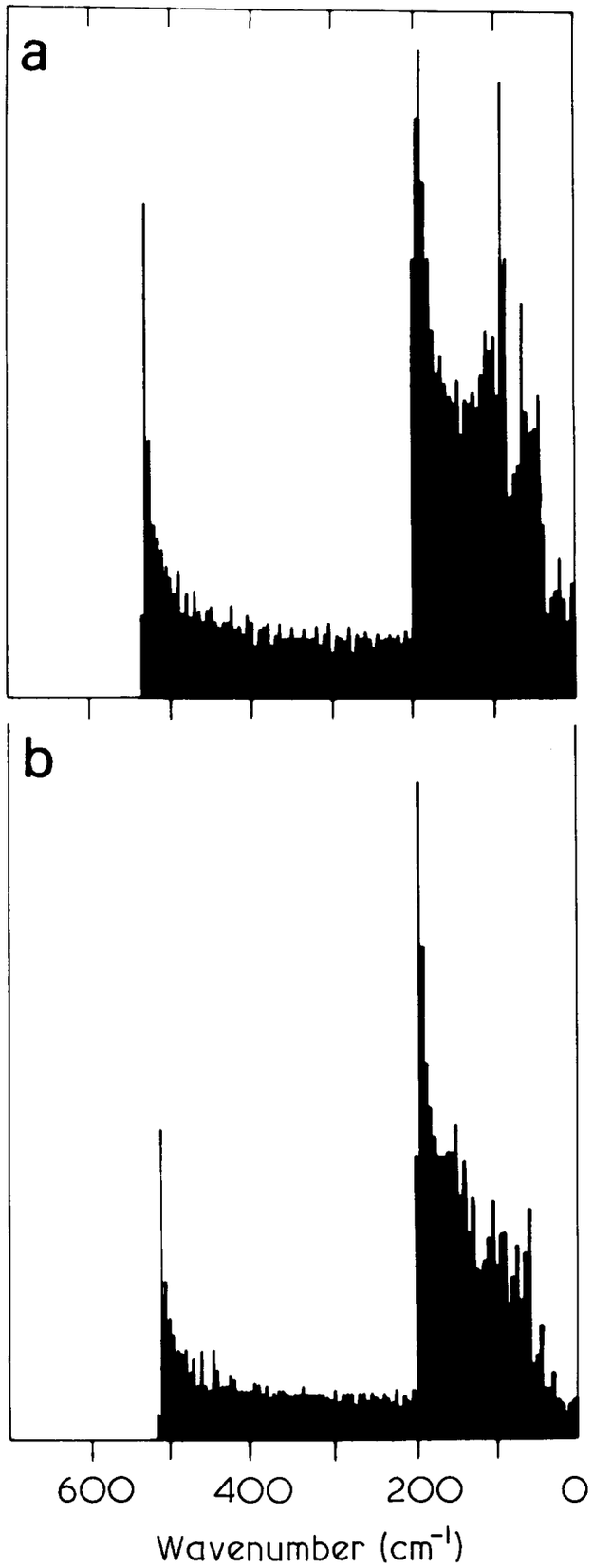

Figure 31 Frequency distribution curves calculated for (a) orthorhombic and (b) monoclinic polyethylene crystals[93]

The calculated vibrational free energy curves for orthorhombic (solid line) and monoclinic (dashed line) forms are shown in *Figure 32*. While the internal energy is not significantly different for both forms, the entropy is significantly higher for orthorhombic form. At 300 K orthorhombic PE has a vibrational free energy of ≈ 0.5 kJ mol^{-1} of methylene unit lower than that of monoclinic PE. The difference is large enough to compensate the higher static potential energy (0.15 kJ mol^{-1} of methylene unit) of the orthorhombic PE, resulting in the thermodynamic stability of this form under normal conditions.

CONCLUSIONS

As has been stated in this paper, the conformations and crystal structures of many polymers have been determined experimentally along with their chemical structures. Based on these studies the prediction of both stable conformations and crystal structures has become possible empirically and theoretically[94]. Basic studies can supply information regarding what types of chemical structures are needed to obtain polymers having certain conformations and crystal structures. Elucidation of the relation of molecular conformation and crystal structure to the fine texture, especially the structure in a wider sense including the structure of the amorphous regions, should

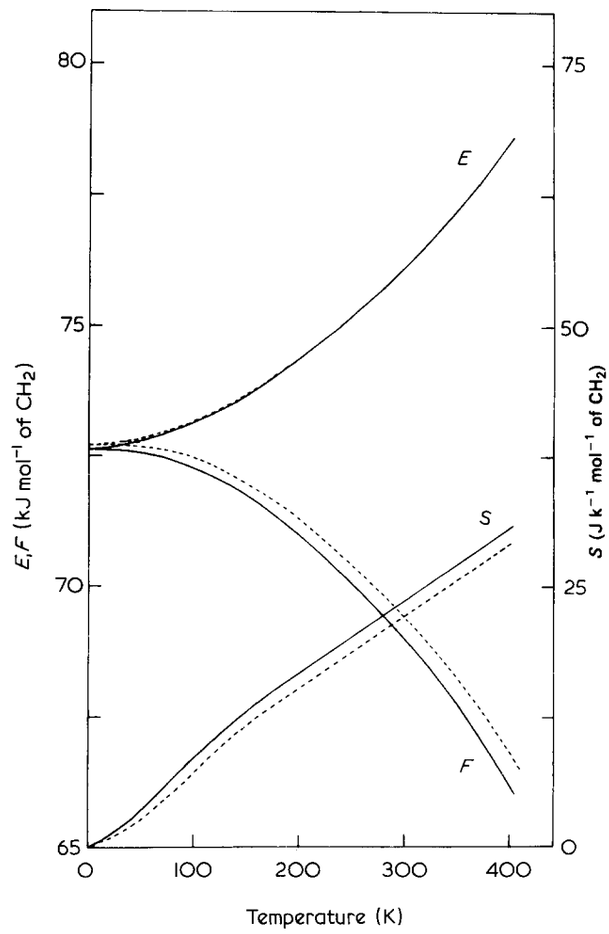

Figure 32 The internal energy *E*, entropy *S*, and Helmholtz free energy *F* calculated for orthorhombic (———) and monoclinic (– – –) polyethylene crystals[93]

provide a deeper understanding of the relation between polymer structure and physical properties such as mechanical, electrical, etc.

ACKNOWLEDGEMENTS

I should like to express my sincere gratitutde to Emeritus Professor Isamu Nitta, Emeritus Professor Shunsuke Murahashi, and Emeritus Professor Shuzo Seki, who have guided and encouraged me throughout my research work. It is a great pleasure that my colleagues and many students from my laboratory have assisted me heartily. I wish also to thank Dr Kohji Tashiro for his assistance in preparing this paper.

REFERENCES

1 Tadokoro, H. *Bull. Chem. Soc. Jpn.* 1955, **28**, 559
2 Tadokoro, H. *Bull. Chem. Soc. Jpn.* 1959, **32**, 1334
3 Tadokoro, H. *J. Polym. Sci.* 1958, **28**, 244
4 Tadokoro, H., Nagai, H., Seki, S. and Nitta, I. *Bull. Chem. Soc. Jpn.* 1961, **34**, 1504
5 Tashiro, K., Kobayashi, M. and Tadokoro, H. *Polym. Bull.* 1978, **1**, 61
6 Tadokoro, H., Nozakura, S., Kitazawa, T., Yasuhara, Y. and Murahashi, S. *Bull. Chem. Soc. Jpn.* 1959, **32**, 313
7 Tadokoro, H., Nishiyama, Y., Nozakura, S. and Murahashi, S. *Bull. Chem. Soc. Jpn.* 1961, **34**, 381
8 Tadokoro, H., Kitazawa, T., Nozakura, S. and Murahashi, S. *Bull. Chem. Soc. Jpn.* 1961, **34**, 1209
9 Huggins, M. L. *J. Chem. Phys.* 1945, **13**, 37
10 Sauter, E. *Z. Physik. Chem.* 1932, **B18**, 417; 1933, **B21**, 186
11 Tadokoro, H., Yasumoto, T., Murahashi, S. and Nitta, I. *J. Polym. Sci.* 1960, **44**, 266
12 Tadokoro, H. *J. Polym. Sci.* 1966, **C15**, 1
13 Uchida, T. and Tadokoro, H. *J. Polym. Sci., A-2* 1967, **5**, 63
14 Takahashi, Y. and Tadokoro, H. *J. Polym. Sci., Polym. Phys. Ed.* 1978, **16**, 1219; 1979, **17**, 123
15 Tadokoro, H. *J. Chem. Phys.* 1960, **33**, 1558
16 Tadokoro, H. *J. Chem. Phys.* 1961, **35**, 1050
17 Tadokoro, H., Kobayashi, A., Kawaguchi, Y., Sobajima, S. and Murahashi, S. *J. Chem. Phys.* 1961, **35**, 369
18 Tadokoro, H., Kobayashi, M., Kawaguchi, Y., Kobayashi, A. and Murahashi, S. *J. Chem. Phys.* 1963, **38**, 703
19 Tadokoro, H., Chatani, Y., Yoshihara, T., Tahara, S. and Murahashi, S. *Makromol. Chem.* 1964, **73**, 109
20 Yoshihara, T., Tadokoro, H. and Murahashi, S. *J. Chem. Phys.* 1964, **41**, 2902
21 Imada, K., Miyakawa, T., Chatani, Y., Tadokoro, H. and Murahashi, S. *Makromol. Chem.* 1965, **83**, 113
22 Imada, K., Tadokoro, H., Umehara, A. and Murahashi, S. *J. Chem. Phys.* 1965, **42**, 2807
23 Tadokoro, H., Takahashi, Y., Chatani, Y. and Kakida, H. *Makromol. Chem.* 1967, **109**, 96
24 Kobayashi, S., Tadokoro, H. and Chatani, Y. *Makromol. Chem.* 1968, **112**, 225
25 Kakida, H., Makino, D., Chatani, Y., Kobayashi, M. and Tadokoro, H. *Macromolecules* 1970, **3**, 569
26 Makino, D., Kobayashi, M. and Tadokoro, H. *J. Chem. Phys.* 1969, **51**, 3901
27 Makino, D., Kobayashi, M. and Tadokoro, H. *Spectrochim. Acta* 1975, **31A**, 1481
28 Takahashi, Y., Sato, T. and Tadokoro, H. *J. Polym. Sci., Polym. Phys. Ed.* 1973, **11**, 233
29 Arnott, S. and Wonacott, A. J. *Polymer* 1966, **7**, 157
30 Takahashi, Y. and Tadokoro, H. *Macromolecules* 1973, **6**, 672
31 Flory, P. J. 'Statistical Mechanics of Chain Molecules' John Wiley & Sons, Inc., New York, 1969
32 Kusanagi, H., Tadokoro, H. and Chatani, Y. *Polym. J.* 1977, **9**, 181
33 Bunn, C. W. and Holmes, D. R. *Discuss. Faraday Soc.* 1958, **25**, 95
34 Tanaka, T., Chatani, Y. and Tadokoro, H. *J. Polym. Sci., Polym. Phys. Ed.* 1974, **12**, 515
35 Natta, G. and Corradini, P. *Nuovo Cimento* 1960, **15**, Suppl., No. 1, 40
36 Tadokoro, H., Tai, K., Yokoyama, M. and Kobayashi, M. *J. Polym. Sci., Polym. Phys. Ed.* 1973, **11**, 825
37 Bassi, I. W., Bonsignori, O., Lorenzi, G. P., Pino, P., Corradini, P. and Temussi, P. A. *J. Polym. Sci., A-2* 1971, **9**, 193
38 Kusanagi, H., Takase, M., Chatani, Y. and Tadokoro, H. *J. Polym. Sci., Polym. Phys. Ed.* 1978, **16**, 131
39 Corradini, P., Ganis, P. and Petraccone, V. *Europ. Polym. J.* 1970, **6**, 281
40 Natta, G., Corradini, P. and Bassi, I. W. *J. Polym. Sci.* 1961, **51**, 505
41 Kusanagi, H., Tadokoro, H., Chatani, Y. and Suehiro, K. *Macromolecules* 1977, **10**, 405
42 Stroupe, J. D. and Hughes, R. E. *J. Am. Chem. Soc.* 1958, **80**, 2341
43 D'alagni, M., De Santis, P., Liquori, A. M. and Savino, M. *J. Polym. Sci., B* 1964, **2**, 925
44 Kusanagi, H., Tadokoro, H. and Chatani, Y. *Macromolecules* 1976, **9**, 531
45 Tadokoro, H., Chatani, Y., Kusanagi, H. and Yokoyama, M. *Macromolecules* 1970, **3**, 441
46 Chatani, Y., Tadokoro, H., Saegusa, T. and Ikeda, H. *Macromolecules* 1981, **14**, 315
47 Chatani, Y., Kobatake, T., Tadokoro, H. and Tanaka, R. *Macromolecules* 1982, **15**, 170
48 Chatani, Y., Kobatake, T. and Tadokoro, H. *Macromolecules* 1983, **16**, 199
49 Kusuyama, H., Takase, M., Higashihata, Y., Tseng, H-To, Chatani, Y. and Tadokoro, H. *Polymer* 1982, **23**, 1256
50 Kusuyama, H., Miyamoto, N., Chatani, Y. and Tadokoro, H. *Polymer* 1983, **24** (*Commun*), 119
51 Sakakihara, H., Takahashi, Y., Tadokoro, H., Oguni, N. and Tani, H. *Macromolecules* 1973, **6**, 205
52 Sakakihara, H., Chatani, Y., Tadokoro, H., Sigwalt, P. and Spassky, N. *Macromolecules* 1969, **2**, 515
53 Yokouchi, M., Chatani, Y., Tadokoro, H., Teranishi, K. and Tani, H. *Polymer* 1973, **14**, 267
54 Yokouchi, M., Chatani, Y., Tadokoro, H. and Tani, H. *Polym. J.* 1974, **6**, 248
55 Takahashi, Y., Tadokoro, H., Hirano, T., Sato, A. and Tsuruta, T. *J. Polym. Sci., Polym. Phys. Ed.* 1975, **13**, 285
56 Matsubayashi, H., Chatani, Y., Tadokoro, H., Dumas, P., Spassky, N. and Sigwalt, P. *Macromolecules* 1977, **10**, 996
57 Dulmage, W. J. and Contois, L. E. *J. Polym. Sci.* 1958, **28**, 275
58 Sakurada, I. *et al. J. Polym. Sci., C* 1966, **15**, 75; 1970, **31**, 57
59 Schaufele, R. F. and Shimanouchi, T. *J. Chem. Phys.* 1967, **47**, 3605
60 Holliday, L. and White, J. W. *Pure Appl. Chem.* 1971, **26**, 545
61 Treloar, L. R. G. *Polymer* 1960, **1**, 95, 279, 290
62 Shimanouchi, T., Asahina, M. and Enomoto, S. *J. Polym. Sci.* 1962, **59**, 93
63 Sugeta, H. and Miyazawa, T. *Polym. J.* 1970, **1**, 226
64 Tashiro, K., Kobayashi, M. and Tadokoro, H. *Macromolecules* 1977, **10**, 731
65 Tashiro, K., Kobayashi, M. and Tadokoro, H. *Macromolecules* 1977, **10**, 413
66 Hasegawa, R. K., Chatani, Y. and Tadokoro, H. Meeting of the Crystallographic Society of Japan, Osaka, Japan, 1973, p. 21
67 Northolt, M. G. *Eur. Polym. J.* 1974, **10**, 799
68 Kaji, K. and Sakurada, I. Kobe Meeting of the Society of Polymer Science of Japan, Kobe, Japan, 1975, p. 56
69 Gaymans, R. J., Tijssen, J., Harkema, S. and Banties, A. *Polymer* 1976, **17**, 517
70 Odajima, A. and Maeda, T. *J. Polym. Sci., C* 1966, **15**, 55
71 Wobser, G. and Blasenbrey, S. *Kolloid Z. Z. Polym.* 1970, **241**, 985
72 Shiro, Y. and Miyazawa, T. *Bull. Chem. Soc. Jpn.* 1971, **44**, 2371
73 Tashiro, K., Kobayashi, M. and Tadokoro, H. *Macromolecules* 1978, **11**, 908
74 Tadokoro, H. 'Recent Developments in Structure Analysis of Fibrous Polymers' (Eds. A. D. French and K. H. Gardner) Am. Chem. Soc. Ser., No. 141, 1980, 43
75 Kobayashi, M. and Tadokoro, H. *J. Chem. Phys.* 1977, **66**, 1258
76 Tashiro, K., Kobayashi, M. and Tadokoro, H. *Macromolecules* 1978, **11**, 914
77 Sakurada, I. and Kaji, K. *Makromol. Chem., Suppl.* 1975, **1**, 599
78 Ito, T. *Polymer* 1982, **23**, 1412
79 Tashiro, K., Tadokoro, H. and Kobayashi, M. *Ferroelectrics* 1981, **32**, 167
80 Tashiro, K. and Tadokoro, H. *Macromolecules* 1981, **14**, 781
81 Tashiro, K., Kobayashi, M. and Tadokoro, H. Symposium on Molecular Structure, Tokyo, Japan, 1979, p. 110

82 Hasegawa, R., Takahashi, Y., Chatani, Y. and Tadokoro, H. *Polym. J.* 1972, **3**, 600
83 Takahashi, Y. and Tadokoro, H. *Macromolecules* 1980, **13**, 1317
84 Davis, G. T., McKinney, J. E., Broadhurst, M. G. and Roth, S. C. *J. Appl. Phys.* 1978, **49**, 4998
85 Davies, G. R. and Singh, H. *Polymer* 1972, **20**, 772
86 Wada, Y. and Hayakawa, R. *Jpn. J. Appl. Phys.* 1976, **15**, 2041
87 Tashiro, K., Kobayashi, M., Tadokoro, H. and Fukada, E. *Macromolecules* 1980, **13**, 691
88 Tashiro, K. and Tadokoro, H. *Macromolecules* 1983, **16**, 961
89 Takahashi, N., Odajima, A., Nakamura, K. and Murayama, N. *Polym. Prepr. Jpn.* 1978, **27**, 364; *Symp. Polym. Electr. Prop.* 1977, 3
90 Bunn, C. W. *Trans. Faraday Soc.* 1939, **35**, 482
91 Seto, T., Hara, T. and Tanaka, K. *Jpn. J. Appl. Phys.* 1968, **7**, 31
92 Yemni, T. and McCullough, L. *J. Polym. Sci., Polym. Phys. Ed.* 1973, **11**, 1385
93 Kobayashi, M. and Tadokoro, H. *Macromolecules* 1975, **8**, 897
94 Tadokoro, H. 'Structure of Crystalline Polymers' Wiley-Interscience, New York, 1979